

1 Tectonic constraints to Cretaceous magmatic arc deduced  
2 from detrital heavy minerals in northeastern Japan -  
3 evidence from detrital garnets, tourmalines and chromian  
4 spinels

5

6 Mayuko Nishio<sup>1</sup> and Kohki Yoshida<sup>2\*</sup>

7

8 <sup>1</sup>J-Power/Electric Power Development Co., LTD., Ghuo-ku, Tokyo, 104-8165, Japan.

9 <sup>2</sup>Department of Geology, Faculty of Science, Shinshu University, Matsumoto, 390-8621,

10 Japan, telephone: +81--263-37-2517, fax: +81-263-37-2506, e-mail:

11 kxyoshid@shinshu-u.ac.jp

12 \* corresponding author

13

14

15

16 **Abstract**

17

18 Tectonic histories of sedimentary basins in the Cretaceous Japan arc  
19 have been assessed to understand the response of the Asian continental margin  
20 to the oblique subduction of the Paleo-Pacific (i.e. Kula or Izanagi) Plate  
21 beneath the Asian continent during the Early Cretaceous and that which  
22 subducted orthogonally in the Late Cretaceous. In the Lower Cretaceous Kuji  
23 Group (Santonian-Campanian) of the Kitakami Massif in northern Japan,  
24 sandstone petrography and chemistry of detrital heavy mineral grains were  
25 performed on sandstones to assess the tectonic environment on the basis of  
26 provenance analysis.

27 Sandstone petrography results suggest that the material of the Kuji  
28 Group was derived mainly from areas of a Cretaceous volcanic belt  
29 (Rebun-Kabato Belt) and from a Jurassic accretionary complex (North Kitakami  
30 Terrane), which was intruded by Cretaceous granite, adjacent to the  
31 depositional basin. The chemical composition of detrital garnets suggests a  
32 North Kitakami Terrane origin, and detrital tourmalines are considered to have  
33 been derived mainly from meta-sedimentary rocks. The composition of detrital  
34 chromian spinels are compositionally diverse and mainly derived from tholeiitic  
35 and intra-plate basalts showing high  $\text{TiO}_2$  (>about 1.0 wt%) and island arc  
36 basalts with moderately low  $\text{TiO}_2$  ( $1.0 > \text{TiO}_2 > 0.5$  wt%) and high  $-\text{Cr}\#$ . Latter

37 chromian spinels can be considered as a record of island arc activity including  
38 high Mg-andesite in Early Cretaceous time. Because adequate source rocks of  
39 the spinels are elusive near the basin compared with those of detrital garnets  
40 and tourmalines, these rocks are believed to have been disturbed by Cenozoic  
41 tectonics and eroded and covered by newly formed volcanic and sedimentary  
42 rocks.

43         Comparison of chemical composition of the chromian spinels between  
44 Lower and Upper Cretaceous deposits in northern Japan indicates that  
45 chromian spinels with very low  $\text{TiO}_2$  (<0.5 wt%) prevail in the Lower Cretaceous  
46 (Aptian-Albian). In contrast, chromian spinels showing moderately low  $\text{TiO}_2$   
47 predominated in the Upper Cretaceous (Santonian-Campanian). This clear  
48 difference suggests the change of oceanic plate motion around Japan arc  
49 promoted the change of source rock assemblage and the arc volcanic activity in  
50 mid-Cretaceous time. Thus the characteristics of detrital heavy mineral  
51 composition of the Kuji Group give the key to clarify the interaction between the  
52 swaying of young and hot plate and development of the Cretaceous island arc in  
53 eastern Asian margin.

54

## 55 **1. Introduction**

56         The success of sandstone petrology in determining the provenance and  
57 tectonic settings of modern and ancient sandstones has been widely documented

58 (Dickinson and Suczek, 1979; Ingersoll, 1978; Dickinson and Valloni, 1980;  
59 Dickinson et al., 1983; Critelli and Ingersoll, 1994, 1995; Critelli and Le Pera,  
60 1994). In recent years, additional effort has been made to relate the composition  
61 of detrital heavy minerals to potential source areas for reconstruction of the  
62 source lithology and paleogeography (Morton, 1985; Hisada et al., 2008). The  
63 combination of sandstone petrography and chemistry of detrital heavy minerals  
64 offers the necessary information for determining the relation between  
65 provenance and major tectonic events.

66         The orthogonal subduction of the Paleo-Pacific (i.e. Kura or Izanagi)  
67 Plate during the Triassic to Late Jurassic transformed to oblique subduction  
68 during the Late Jurassic to Early Cretaceous (Chang, 1995; Lithgow-Bertelloni  
69 and Richards, 1998). This northward oblique subduction led to major tectonic  
70 events such as arc magmatism, orogeny, and sinistral shearing in the overriding  
71 continental plate in the Early Cretaceous period. As a result, many strike-slip  
72 basins trending northeast–southwest were formed in the East Asian continental  
73 margin (Maruyama and Seno, 1986; Maruyama et al., 1997; Okada and Sakai,  
74 2000). Furthermore, from 90 Ma to the end of the Cretaceous, the oceanic plate  
75 was moving to the west and an oceanic ridge that existed between the  
76 Izanagi–Kula Plate and the Pacific Plate subducted beneath the Asian  
77 continent near southwestern Japan (Maruyama et al., 1997). The change of  
78 plate motion with high speed subduction of the young and buoyant oceanic plate

79 generated remarkable igneous activity (Takahashi, 1983; Maruyama and Seno,  
80 1986; Tsuchiya et al., 2005, 2007). Thus, tectonics in the eastern marginal area  
81 of the Asian continent, which includes the Japanese islands, eastern China, the  
82 Korean peninsula, and Far East Russia, is characterized by magmatism and  
83 metamorphism caused by swaying plate motion of the young and buoyant  
84 oceanic plate with high speed convergence.

85         The Kuji Basin is a small Cretaceous basin in the northern Japanese  
86 islands. The Cretaceous sedimentary rocks deposited in this basin could contain  
87 a record of specific tectonics related to the subduction of hot and young oceanic  
88 plates during Cretaceous, because the depositional duration of the Kuji Group  
89 show considerable overlap with change of oceanic plate motion shown by  
90 Maruyama and Seno (1986) and Maruyama et al. (1997). This paper reports the  
91 petrography and chemistry of heavy mineral grains in the sandstones of the  
92 Lower Cretaceous Kuji Group (Shimazu and Teraoka, 1962) distributed in the  
93 Kitakami Massif in northern Japan (Fig. 1). In this study, in order to clarify the  
94 tectonic influence of the transition of Cretaceous plate motion, we discuss the  
95 chemistry of garnet, tourmaline, and chromian spinel detrital grains; these  
96 heavy minerals are important accessory minerals in metamorphic and  
97 mafic-ultramafic rocks (Dick and Bullen, 1984; Arai and Okada, 1991; Morton  
98 and Hallsworth, 1999; Barnes and Roeder, 2001; von Eynatten, 2003; Yoshida et  
99 al., 2010).

100

## 101 **2. Geological setting**

102           The Kuji Group is located in the northern part of the Kitakami Massif  
103 which primarily consists of a Jurassic accretionary complex known as North  
104 Kitakami Terrane and Lower Cretaceous granites. The Kuji Group  
105 unconformably overlies these pre-Upper Cretaceous units (Shimazu and  
106 Teraoka, 1962) and is disconformably overlain by the Paleogene Noda Group  
107 (Figs. 2 and 3).

108           The Kuji Group is approximately 400 m thick and consists of the  
109 Tamagawa, Kunitan, and Sawayama formations in ascending order. The  
110 Tamagawa Formation is probably Santonian in age (Miki, 1977). The  
111 stratigraphy is constrained by *Inoceramus*, mainly from the Kunitan Formation,  
112 and is assigned to the Santonian (Terui and Nagahama, 1995). A zircon fission  
113 track age of  $71.2 \pm 14.4$  Ma reported from a felsic tuff in the Sawayama  
114 Formation suggests a Campanian age (Kato et al., 1986). Clay mineral  
115 assemblages and vitrinite reflectance of carbonaceous matter indicate  
116 diagenetic palaeotemperatures below 50 °C (Kimura et al., 2005). The age of the  
117 Noda Group was determined as early Oligocene from plant fossil data (Shimazu  
118 and Teraoka, 1962).

119

### 120 **2.1 Tamagawa Formation**

121           The Tamagawa Formation reaches a maximum thickness of 80 m and  
122 gradually thins toward the northwest. The lithofacies consists of a basal breccia  
123 conglomerate followed by cross-bedded sandstone with coal seams and *Ostera*  
124 beds. In the middle part, alternating beds of cross-bedded granule–pebble  
125 conglomerate and cross-bedded sandstone with burrows prevail. Alternating  
126 beds of conglomerate, sandstone, and mudstone with coal seams and rootlets  
127 dominate the upper part. The modal composition of the conglomerate outcrops  
128 exhibits dominant framework constituents of sandstone and chert clasts  
129 (Shimazu and Teraoka, 1962; Nagahama and Terui, 1977).

130

## 131 **2.2 Kunitan Formation**

132           The Kunitan Formation is approximately 170 m thick and mainly  
133 comprises marine sandstone and mudstone. The lithology includes cross-bedded  
134 very fine- to medium-grained sandstone in the lower part, HCS (Hummocky  
135 cross stratification) fine-grained sandstone in the middle part, and medium- to  
136 coarse-grained cross-bedded sandstone in the upper part. Mesozoic-derived  
137 sedimentary and meta-sedimentary clasts are dominant and include chert,  
138 sandstone, and hornfels in the conglomerate and significant amounts of volcanic  
139 clasts in the lower part (Nagahama and Terui, 1977). The lower part of this  
140 formation is focused in the present study.

141

### 142 **2.3 Sawayama Formation**

143           The Sawayama Formation consists of fluvial conglomerate, cross-bedded  
144 sandstone, mudstone with tuff, and coal beds. This formation is not focused in  
145 the present study.

146

### 147 **2.4 Sedimentary environment**

148           Following Terui and Nagahama (1995), several sedimentary facies were  
149 reported from the Kuji Group that includes deposits from alluvial fans, fluvial  
150 channel fills, flood plains, coastal dunes, lagoon, foreshore, upper and lower  
151 shorefaces, and the inner shelf. During the deposition of the lower part of the  
152 Tamagawa Formation, an initial fluvial depositional environment changed to  
153 that of foreshore–upper shoreface. The detritus was derived from variable  
154 directions by an extensive alluvial fan or river system. In the period of  
155 deposition of the middle and upper parts of the Tamagawa Formation, the  
156 environment changed from fluvial to upper shoreface before finally returning to  
157 fluvial. In the Kunitan Formation, the sedimentary environment changed from  
158 upper shoreface to lagoon with thick fossil beds of oysters. The Sawayama  
159 Formation was deposited in a fluvial environment with detritus derived mainly  
160 from the north.

161

### 162 **3. Methods**

163 Thirteen sandstone samples spanning the entire stratigraphic section  
164 were collected from the Tamagawa and Kunitan formations for the provenance  
165 study (Fig. 4). These formations do not exhibit intense deformation by  
166 post-depositional tectonics although the bedding plane gently declines to the  
167 east. Thus, the diagenetic alteration by compaction and deformation is minimal.

168 Fresh rock exposures are abundant and readily accessible for sampling  
169 along the Tamagawa coast (Fig. 2). Medium-grained sandstone samples were  
170 selected for thin- and polished-section studies. Modal analysis of seven thin  
171 sections was performed using the Gazzi–Dickinson point-counting technique  
172 (Dickinson and Suzeck, 1979) and included more than 500 points per thin  
173 section. For chemical analysis of the heavy minerals, the sandstone was crushed  
174 in an iron bowl and sieved, and the heavy mineral grains were separated using  
175 a heavy liquid (SPT: sodium polytungstate) and glued onto a thin section with  
176 epoxy resin. All thin sections were subsequently polished and carbon coated.  
177 Chemical analysis of the selected mineral grains, i.e., garnet, tourmaline, and  
178 chromian spinel, was established with an EDS (JEOL-5033) microprobe  
179 analyzer at the Faculty of Science, Shinshu University, Japan. Operating  
180 conditions included an acceleration voltage of 15 kV, probe current of 720 pA,  
181 counting time of 120 s per specimen, and beam diameter of 20  $\mu\text{m}$ .

182

#### 183 **4. Results**

#### 184 4.1 Sandstone petrography

185 Point-counting results are shown in Table 1 and Fig. 5 as Qm–F–Lt and  
186 Q–F–L ternary diagrams. The sandstones of the Kuji Group are characterized  
187 by a high amount of rock fragments consisting of rhyolite, rhyolitic tuff,  
188 andesite, chert, and granite (Figs. 6-A, B). The matrix of the sandstones is less  
189 than 1%; however, the cement component of carbonates and clay minerals is  
190 between 0% and 13%. No compositional variation is evident in the sandstone  
191 mode, owing to differences in the sampling horizons.

192 Quartz grains generally comprise 6%–15% of the modal composition  
193 with monocrystalline quartz grains in higher abundance than polycrystalline  
194 quartz grains. The latter mainly consist of nonoriented grains with straight to  
195 undulose extinction and straight grain boundaries; however, rare orientated  
196 quartz grains were also observed. The monocrystalline quartz grains are  
197 euhedral with nonundulatory extinction; small embayments, fewer inclusions,  
198 and clear transparency indicate volcanic origin. Several quartz crystals of this  
199 type mostly contain inclusions of white mica, biotite, and opaque minerals.

200 Feldspar grains, which are rare in the sandstone, are subhedral to  
201 euhedral with a slightly higher abundance of plagioclase grains over those of  
202 potassium feldspar. Several plagioclase grains are fresh and unaltered;  
203 nonetheless, most plagioclase are replaced with carbonates or altered to clay  
204 minerals. Potassium feldspar, which includes orthoclase, was distinguished

205 from quartz by the presence of cleavage, cloudy alteration, and lower refractive  
206 indices. Microcline and microperthite were observed in a few samples.

207 Lithic volcanic clasts comprise 60%–80% of the modal composition and  
208 are the predominant component in all analyzed samples. Most clasts are felsic  
209 and aphanitic volcanic rock fragments. The felsic volcanic clasts, which include  
210 small euhedral plagioclase grains within an aphanitic matrix, are abundant.  
211 Vitric and vitroclastic volcanic clasts also occur and have a groundmass  
212 consisting mainly of altered and devitrified glass. Grains with pseudomorphs of  
213 glass shards and flow structures were observed in some samples. The mafic  
214 volcanic fragments, which mostly show a microlitic texture with plagioclase  
215 laths in an altered aphanitic groundmass, are rare. Irregular opaque fragments  
216 have been interpreted as volcanic mafic fragments owing to the occasional  
217 appearance of plagioclase and mafic mineral inclusions (Critelli and Ingersoll,  
218 1995; Critelli et al., 2002). Meta-sedimentary rock fragments, which originated  
219 from sandstones and mudstones, occasionally contain small euhedral biotite  
220 grains, suggesting the effects of thermal metamorphism. Chert grains mostly  
221 exhibit the effects of thermal metamorphism through mosaic textures with  
222 coarse euhedral quartz grains. Rare red-colored chert grains include both  
223 microcrystalline and pseudomorphs of radiolarian fossils. Microcrystalline chert  
224 grains were distinguished from microcrystalline felsic volcanic rock fragments  
225 by a lack of marked internal relief between individual crystals, a lack of

226 feldspar microphenocrysts, and the occasional presence of crisscrossing veinlets.

227         Accessory minerals such as zircon, garnet, biotite, epidote, chlorite,  
228 tourmaline, clinopyroxene, hornblende, and chromian spinel are evident in the  
229 sandstone.

230

#### 231 **4.2 Heavy minerals**

232         After the separation procedure, the heavy minerals, in decreasing order  
233 of abundance, are epidote, Fe–Ti oxides (i.e., magnetite and ilmenite), chlorite,  
234 garnet, chromian spinel, zircon, rutile, titanite, tourmaline, hornblende, and  
235 pyroxenes.

236         The detrital garnets of the Kuji Group mostly occur as small angular  
237 fragments of 0.05-0.2 mm in diameter (Fig. 6-C). Round or euhedral grains are  
238 generally rare. The garnets are mostly colorless, though some reddish green,  
239 pinkish green, and pale green varieties were observed. Zircons, 0.03-0.1 mm in  
240 diameter, are mostly euhedral and angular, either well-rounded or subrounded.  
241 Epidote grains are mostly irregular and angular and 0.05-0.1 mm in diameter.  
242 The detrital titanite grains in the sandstones are mostly fine and red in color,  
243 euhedral to irregular, and mostly free of inclusions. Most tourmaline grains are  
244 subround to subhedral and 0.1-0.3 mm in diameter. In the thin section, these  
245 grains occur in shades of green, greenish yellow, greenish blue, pale green,  
246 reddish yellow, and yellow (Fig. 6-D). Chromian spinel grains are mostly

247 reddish brown; however, a few grains are dark brown or black. The grain size  
248 and shape have wide variety from 0.3 mm to 0.03 mm in diameter and from  
249 angular to sub-angular. Several grains are found with euhedral shape (Figs. 6-E  
250 and F).

251

#### 252 **4.2.1 Detrital garnet**

253 All analyses were performed at the core of the grains. The molecular  
254 endmembers were calculated using the method of Deer et al. (1992).  
255 Representative analyses of the detrital garnets are listed in Table 2, and the  
256 compositional data are illustrated in Fig. 7. The chromium contents in all cases  
257 were below or close to the detection limits, and the oxide totals were close to  
258 100%. Thus, the contribution of the uvarovite and hydrogrossular garnet  
259 endmembers can be ignored. The compositions of the detrital garnets can be  
260 expressed in terms of the following endmembers: almandine, pyrope,  
261 spessartine, grossular, and andradite. The garnets are rich in FeO\* (16.8–21.6  
262 wt%, average 20.2 wt%), and poor in Cr<sub>2</sub>O<sub>3</sub> (less than 0.26 wt%) and TiO<sub>2</sub> (less  
263 than 0.80 wt%). The MgO content range is 2.80–8.67 wt% (average 2.77 wt%).  
264 The MnO content is generally erratic and can reach a maximum of 20.0 wt%.  
265 The CaO content is generally low and erratic. Although its maximum is 31.0  
266 wt%, the content is mostly below 7.0 wt%. The chemical composition of the  
267 garnet grains varies; however, the pyrope–almandine component dominates,

268 followed by spessartine–almandine. Grossular component is relatively minor.

269

#### 270 **4.2.2 Detrital Tourmaline**

271 Detrital tourmaline varies widely in grain size and grain shape, and its  
272 color is green, greenish yellow, greenish blue, pale green, reddish yellow, and  
273 yellow. The chemical composition also varies widely (Table 3). The  
274 Al–Fe–Mg–Ca-discrimination diagrams of Henry and Guidotti (1985) allow for  
275 excellent assignment of many different source rocks. Among the detrital  
276 tourmalines, the meta-sedimentary tourmalines predominate over those of  
277 magmatic origin from granitic or associated pegmatitic sources (Fig. 8). The  
278 magmatic tourmalines contain a higher Mn content (0.10–0.56 wt% MnO;  
279 0.01–0.08 Mn p.f.u.) than those derived from a meta-sedimentary source. The  
280 tourmalines from a meta-psammopelitic source vary widely in the Al–Fe–Mg  
281 diagram covering Al-rich metapelites and metapsammites, Al-poor metapelites  
282 and metapsammites, and Fe<sup>3+</sup>-rich metapelites and calc-silicate rocks. Ca-poor  
283 metapsammopelites predominate in the Tamagawa and Kunitan formations,  
284 with the exception of one grain within the field of meta-ultramafics. The  
285 distribution of the tourmaline compositions in the Kuji Group does not depend  
286 on the sampling horizon.

287

#### 288 **4.2.3 Detrital chromian spinel**

289 To determine compositional variations within grains, we analyzed the  
290 core and rim of all the grains. No compositional variations were observed either  
291 by microscope or electron microprobe. The chromian spinel composition varies  
292 widely (Table 4) with a  $\text{Cr}_2\text{O}_3$  content range of 23.8–60.6 wt%; however, most of  
293 the grains show contents greater than 30.0 wt%. The  $\text{Al}_2\text{O}_3$  content range is  
294 3.37–39.2 wt%, averaging 12.0 wt%.  $\text{Cr}_2\text{O}_3$  and  $\text{Al}_2\text{O}_3$  show weak negative  
295 correlation. The  $\text{FeO}^*$  range of 16.1–45.8 wt% negatively correlates with the  
296  $\text{MgO}$  range of 0–16.7wt%, averaging 7.52 wt%.  $\text{MnO}$  is low with a range of  
297 0.42–2.35 wt%. The  $\text{TiO}_2$  content range is 0.17–5.50 wt%. The  $\text{Fe}^{3+}/(\text{Fe}^{3+}+\text{Al}+\text{Cr})$   
298 ratio ranges from 0.01 to 0.32; the  $\text{Cr}/(\text{Cr}+\text{Al})$  ratio ( $\text{Cr}\#$ ) ranges from 0.29 to  
299 0.92 with an average of 0.72; and the  $\text{Mg}/(\text{Mg}+\text{Fe}^{2+})$  ratio ( $\text{Mg}\#$ ) ranges widely  
300 from 0 to 0.78 with an average of 0.37.

301 No compositional bias by sedimentary environments (Fig. 9-A) is  
302 apparent. On the basis of the  $\text{TiO}_2$ – $\text{Cr}\#$ : $\text{Cr}/(\text{Cr}+\text{Al})$  diagram by Arai (1992) (Fig.  
303 9-B), we identified three broad categories: tholeiitic-intra-plate basalt group  
304 showing moderate  $\text{Cr}\#$  ( $<0.8$ )–high  $\text{TiO}_2$  ( $>1.0$  wt%); island arc basalt group  
305 showing high  $\text{Cr}\#$  ( $>0.6$ )–moderately low  $\text{TiO}_2$  ( $0.15<\text{TiO}_2<1.0$  wt%); and  
306 intra-plate basalt group showing low  $\text{Cr}\#$  ( $<0.6$ )–moderately high  $\text{TiO}_2$  ( $<1.0$   
307 wt%). The very low  $\text{TiO}_2$  spinels showing moderate  $\text{Cr}\#$  ( $>0.6$ )–very low  $\text{TiO}_2$   
308 ( $<0.15\text{wt}\%$ ) are not distinguished as a group, because of only three grains.  
309 Tholeiitic-Intra-plate basalt group corresponds to tholeiitic and intra-plate

310 basalts fields; island arc basalt group is mainly plotted in an island arc basalt  
311 field in close proximity boninite fields; very low TiO<sub>2</sub> grains is plotted near  
312 island arc basalt and boninites fields. In the Al<sub>2</sub>O<sub>3</sub>–TiO<sub>2</sub> diagram of  
313 Kamenetsky et al. (2001), spinels concentrate in arc and oceanic island basalt  
314 fields with some spinel compositions in the MORB and SSZ peridotite fields (Fig.  
315 9-C). In the ternary Fe<sup>3+</sup>–Cr–Al diagram (Fig. 9-D), the spinel compositions fall  
316 within the wide area of the boninite and island-arc fields of Barnes and Roeder  
317 (2001). Some of the high Cr# spinels are plotted in modern boninite fields in the  
318 Chichijima Izu–Mariana arc (Yajima and Fujimaki, 2001), as shown in Fig. 9-A.

319

## 320 **5. Pre-Late Cretaceous rocks in the Kitakami Massif**

321 The pre-Cretaceous rocks in northern Japan, particularly in the  
322 Kitakami Massif, are a potential source of detritus of the Kuji Group Basin and  
323 include North Kitakami, South Kitakami, and Nedamo Terranes. In addition,  
324 the Lower Cretaceous volcanic rocks called as the Harachiyama Formation on  
325 the North Kitakami Terrane, Lower Cretaceous volcanics and sedimentary  
326 rocks on the Nedamo and South Kitakami Terranes and Lower Cretaceous  
327 granites are also candidate members. A simplified stratigraphic column is  
328 shown in Fig. 10, and a brief review of these rocks is given in this section.

329 The North Kitakami Terrane, which is located in the northern part of  
330 the Kitakami Massif, is a mélangé with a matrix of terrigenous clastic rocks and

331 blocks in addition to fragments of Carboniferous to Permian basalts and  
332 limestones originating from seamounts and Carboniferous to Middle Jurassic  
333 pelagic cherts (Okami and Ehiro, 1988; Minoura, 1990; Ehiro et al., 2008).

334         These rocks are unconformably overlain by various Lower Cretaceous  
335 volcanic and volcanoclastic rocks comprising the 3500-m-thick, island arc  
336 volcanic rocks (Harachiyama Formation), which mainly consists of dacite,  
337 rhyolite, and basalt with various pyroclastic and tuffaceous rocks (Shimazu,  
338 1979). The sedimentary rocks linked to this formation yield  
339 Hauterivian–Barremian plant and mollusk fossils (Yamaguchi et al., 1979;  
340 Matsumoto et al., 1982).

341         The South Kitakami Terrane consists of Paleozoic–Lower Cretaceous  
342 rocks deposited on pre-Silurian granites and ultramafic rocks (Yoshida and  
343 Machiyama, 2004). This terrane is considered to be continental fragments  
344 accreted to Japan arc during Cretaceous time (Saito and Hashimoto, 1982).

345         The Neadamo Terrane, which is a Paleozoic accretionary complex, is  
346 situated between the northwestern margin of the South Kitakami Terrane and  
347 the southern margin of the North Kitakami Terrane. This complex consists of  
348 alternating beds of mudstones and felsic tuffs, thick felsic tuffs, and oceanic  
349 greenstones with minor cherts, mudstones, sandstones, conglomerates, and  
350 gabbros (Uchino et al., 2005). Late Devonian conodonts have been discovered in  
351 the red cherts (Hamano et al., 2002) and 380-Ma-old high-P/T schists

352 (Kawamura et al., 2007) were reported. Thus the accretionary age is assigned to  
353 Early Carboniferous (Uchino et al., 2005). This complex is severely sheared and  
354 intruded by numerous serpentinite bodies along faults.

355 The pre-Upper Cretaceous sequences were intruded and  
356 metamorphosed by Lower Cretaceous granites (Kawano and Ueda, 1967). The  
357 radiometric ages of the granites are 110–121 Ma (Shibata et al., 1978). The  
358 granites thermally metamorphosed all the pre-Upper Cretaceous rocks.

359 Finally, Lower Cretaceous, Aptian–Albian fossiliferous shallow marine  
360 deposits known as the Miyako Group, which are sporadically distributed along  
361 the present coastline as small bodies, lie unconformably over various types of  
362 sedimentary and volcanic rocks of the North Kitakami Terrane and  
363 Harachiyama Formation, and Lower Cretaceous granites (Hanai et al., 1968).

364

## 365 **6. Probable source rocks**

### 366 **6.1 Sandstone composition**

367 The general lithic and immature nature of the sandstones in the Kuji  
368 Group, characterized by a high amount of volcanic lithic fragments and low  
369 quartz and feldspar contents, suggests short transport distance with the source  
370 areas in close proximity to the depositional basin. The high proportion of glassy  
371 volcanic rock fragments also suggests significant contribution from volcanic  
372 rocks, related to active volcanism during sedimentation and pre-existed volcanic

373 terrane. The volcanic supply is interpreted here as related to paleovolcanic  
374 provenance and subordinate neovolcanic provenance (e.g., Critelli and Ingersoll,  
375 1995; Critelli et al., 2002; Caracciolo et al., 2011). Rare phenocrysts of  
376 potassium feldspars indicate limited contribution of rhyolites. Scarce  
377 fine-grained sedimentary lithic fragments, chert, and rounded zircon grains  
378 suggest minor contributions from sedimentary rocks. The Lower Cretaceous  
379 volcanic rocks, the Harachiyama Formation, which consists of dacite, rhyolite  
380 and basalt, are distributed around the basin (Sasaki and Tsuchiya, 1999).  
381 Though this volcanic formation is perhaps the parent of the volcanic rock  
382 fragments, detrital chromian spinels with euhedral shape probably suggest the  
383 mafic volcanic rocks including chromian spinel phenocryst. Contact  
384 metamorphic rocks created by the Lower Cretaceous granites are also  
385 considered as sources of the metamorphosed sedimentary rock fragments  
386 because fresh chert grains with radiolarian pseudomorphs indicate a sediment  
387 supply from an accretionary complex. The minor amounts of basaltic volcanic  
388 rock fragments were likely supplied from the greenstones in the North  
389 Kitakami Terrane, which is consistent with the origin of the chromian spinels  
390 from tholeiite basalts. The presence of biotite grains suggests the occurrence of  
391 granitic or rhyolitic rocks in the hinterland.

392

## 393 **6.2 Heavy minerals**

394           The provenance area for the detrital garnets cannot be tightly  
395 constrained owing to a limited amount of detrital garnet data. Nakamoto et al.  
396 (1996) suggested that the sandstones in the Jurassic accretionary complex  
397 contain detrital pyrope-rich almandine garnets and Ca–Mn-rich almandine  
398 garnets (Fig. 7). The sources of these garnets are likely metamorphosed  
399 mudstones and calcareous sedimentary rocks (Miyashiro, 1953; Coleman et al.,  
400 1965; Deer et al., 1992). Furthermore, Ca–Mn-rich almandine garnets have  
401 compositional similarity to high-P type metamorphic rocks (Coleman et al.,  
402 1965), Ca-rich amphibolite (Inazuki, 1981) and skarn (Einaudi and Burt, 1982).  
403 However, high-grade metamorphic rocks were not observed near the Kitakami  
404 Massif. Thus, the detrital pyrope-rich and Ca–Mn-rich almandine garnets in  
405 the Kuji Group were likely supplied by the sandstones of the North Kitakami  
406 Terrane. The grossular-rich garnets, which are a minor component of the  
407 detrital garnets in the Kuji Group sandstones, were possibly derived from the  
408 sandstones of the North Kitakami Terrane complex or low-grade metamorphic  
409 rocks that originated from the mudstones and calcareous sedimentary rocks of  
410 the North Kitakami Terrane after contact metamorphism.

411           The potential of detrital tourmaline compositions in provenance studies  
412 lies in their direct comparison with those from suspected source lithologies. The  
413 thermally metamorphosed sedimentary rocks and pegmatites from the Lower  
414 Cretaceous granites are the most likely sources for the detrital tourmalines.

415 The tourmalines from meta-sedimentary rock predominate, which indicates  
416 that distribution of the pegmatites was limited in the hinterland, and the  
417 meta-sedimentary rocks were an abundant source of tourmalines. However,  
418 considering that the detrital garnets originated from the sandstones in the  
419 North Kitakami Terrane, it is probable that the sandstones in the North  
420 Kitakami Terrane also supplied the tourmaline grains to the Kuji Basin.

421         Of the detrital chromian spinels shown in Fig. 9-B, spinels with  
422 moderate Cr# and high TiO<sub>2</sub>, were most likely supplied from intra-plate basalts  
423 including alkaline and tholeiitic basalts, whereas those in the North Kitakami  
424 Terrane show good correlation to oceanic basalts (Miura and Ishiwatari, 2001).  
425 Spinel with high Cr# and moderately low TiO<sub>2</sub>, is concentrated between  
426 island-arc basalt and boninite fields. The nature of the high Cr#–relatively low  
427 TiO<sub>2</sub> and low Fe<sup>3+</sup>/(Fe<sup>3+</sup>+Cr+Al) ratio also indicates derivation from island arc  
428 basalt and boninite (Barnes and Roeder, 2001); however, no correlative lithology  
429 is evident near the basin. The source rocks of this type are further discussed in  
430 next section. Spinel with high Cr# and very low TiO<sub>2</sub>, suggest derivation from  
431 boninite and ultramafic rocks, possibly the Nedamo Terrane. The present  
432 distribution of the northern margin of the Nedamo Terrane, however, is more  
433 than 60 km south of the basin of the Kuji Group. In addition, the chemistry of  
434 those chromian spinels contained in serpentinite bodies, showing very low TiO<sub>2</sub>  
435 wt% from 0 to 0.6 and wide variety of Cr# from 0.05 to 0.8 (Fujimaki and

436 Yomogida, 1986a, 1986b), is different from chemical characteristics of detrital  
437 spinels in the Kuji Group. Thus, a suitable source lithology remains elusive.

438 Another possibility is recycled spinels from the Jurassic sandstones in  
439 the North Kitakami Terrane; however, it is unlikely that the detrital spinels in  
440 the Kuji Group are recycled origin, because the spinels show angular and  
441 euhedral grain shapes.

442

#### 443 **7. Provenance and tectonic setting of the Kuji Group**

444 The data from sandstone petrography can indicate the ancient tectonic  
445 setting of a depositional basin. The petrography of the sandstones in the Kuji  
446 Group suggests undissected - transitional volcanic arc provenances, mainly  
447 from glassy volcanic rocks. However, the chemistry of the detrital garnets  
448 suggests derivation from contact metamorphic rocks adjacent to the Lower  
449 Cretaceous granites and sandstones in the North Kitakami Terrane. The  
450 chemistry of the tourmaline grains also suggests an origin of granites,  
451 pegmatites, and meta-sedimentary rocks from contact aureoles. These origins  
452 are consistent with the clast composition results of the conglomerate in the Kuji  
453 Group (Nagahama and Terui, 1977) and of previous petrographic research  
454 (Okami et al., 1994) although the origin of chromian spinels remains obscure.

455 Because the Kuji Group unconformably overlies the Cretaceous granites  
456 in several areas, it is likely that most of the detritus was derived from the

457 sedimentary rocks and metasedimentary rocks acting as roof rocks on the  
458 granites. Accordingly, the vast volume of these roof rocks intruded by the  
459 granites was eroded away to sufficiently expose the granite prior to the  
460 deposition of the Kuji Group.

461         The distribution of a positive magnetic anomaly zone was reported to  
462 coincide with the Cretaceous volcanic rocks of the Rebun-Kabato Belt and  
463 plutonic rocks extending from Hokkaido Island to the offshore side of the Kuji  
464 Basin (Segawa and Furuta, 1978; Osawa et al., 2002). Thus, the Cretaceous  
465 volcanic rocks of the Rebun-Kabato Belt (Fig. 1-B) are possibly distributed to  
466 the eastern side of the basin, where they are present in the offshore area,  
467 although newly formed volcanic and sedimentary rocks may have concealed  
468 them. Indeed, Cretaceous mafic volcanic rocks were retrieved as cuttings from  
469 the bottom of the drill hole to the northeast of the Kuji (Japan Natural Gas  
470 Association and Japan Offshore Petroleum Development Association, 1992) and  
471 the Oligocene deposits unconformably overlie on the Cretaceous deposits to the  
472 east of the Kuji Basin (ex. Arthur et al., 1980). Nagata et al. (1986) suggested  
473 that the magmatism of the Rebun-Kabato Belt is mainly tholeiitic and  
474 calc-alkalic, and Sasaki and Tsuchiya (1999) reported a magmatic resemblance  
475 of the volcanic rocks between the Rebun-Kabato Belt and the Cretaceous  
476 volcanic rocks, the Harachiyama Formation near Kuji Basin. This volcanic belt  
477 is considered to have formed in Berriasian-Cenomanian time, designating

478 before onset of the Kuji Group, on the basis of radiometric ages of volcanic rocks  
479 and radiolarian fossils from mudstones intercalated in the volcanic rocks  
480 (Nagata et al., 1986; Kondo, 1993). Furthermore the age of the Harachiyama  
481 Formation is 93-119 Ma (Shibata et al., 1978) and Upper Cretaceous,  
482 Campanian- Maastrichtian volcanic rocks, which have yielded radiometric age  
483 of  $71.3 \pm 2.4$  Ma ( $^{40}\text{Ar}$ - $^{39}\text{Ar}$  dating), were also reported (Takigami, 1991).  
484 Therefore, the volcanic fragments included in the sandstones of the Kuji  
485 Formation are believed to originate mainly from the Cretaceous volcanic rocks  
486 which correlate with those in the Rebun-Kabato Belt to the east of the basin. In  
487 such circumstances, the island-arc type chromian spinels, plotted in island arc  
488 basalts field in Fig. 9-B, could have been provided from part of the  
489 Rebun-Kabato Belt. A schematic illustration of the relationship between  
490 provenance and the basin is shown in Fig. 11.

491

## 492 **8. Comparison of chromian spinel composition with Lower Cretaceous deposits** 493 **in northern Japan**

### 494 **8.1 Compositional change of chromian spinel between the Lower and Upper** 495 **Cretaceous deposits**

496 The Yezo Group, which is distributed in the central part of Hokkaido  
497 Island (Fig. 1-B), is known as Cretaceous forearc basin deposits along with the  
498 Kuji Group in northern Japan (Kimura, 1994; Ando, 2003). The detrital

499 chromian spinels and serpentine-bearing conglomerate were reported from  
500 several horizon of the Yezo Group by Nanayama (1997), Nanayama et al. (1997)  
501 and Yoshida et al. (2003, 2010). These studies suggest that the chromian spinels  
502 in the Yezo Group are mainly characterized by the very low  $\text{TiO}_2$  wt% (<0.5  
503 wt%) spinels with minor amount of high  $\text{TiO}_2$  (>0.5 wt%) spinels (Fig. 12). The  
504 chemical characters of chromian spinels in the Yezo Group indicate the  
505 derivation from peridotites of arc or forearc setting (Yoshida et al., 2003, 2010).

506 On the other hand, the predominance of the chromian spinels with  
507 moderately low  $\text{TiO}_2$  in the Kuji Group shows significant difference from the  
508 Lower Cretaceous (Aptian - Albian) deposits, for example, Kamiiji Formation in  
509 the Yezo Group (Yoshida et al., 2010, Taki et al., 2011; Fig. 12). The moderately  
510 low  $\text{TiO}_2$  content and euhedral shape of the chromian spinels in the Kuji Group  
511 are indicative to the derivation mainly from island arc volcanic rocks. This  
512 compositional difference in detrital chromian spinels possibly shows the  
513 provenance change around Japanese islands in Mid-Cretaceous period.

## 514 **8.2 Relationship between the compositional change of chromian spinels and** 515 **tectonics at the Japanese islands in the Cretaceous**

516 It is known that the Japan arc were located along the eastern margin of  
517 the Asian continent in Cretaceous time (Taira and Tashiro, 1987) and the  
518 Izanagi plate moved northward with oblique subduction around Early  
519 Cretaceous. The rapid plate motion developed transcurrent movement that

520 might have linked to faulting activity with serpentinite infiltration in forearc  
521 region of Japanese islands in Early Cretaceous times (Hisada et al., 1999). The  
522 chromian spinels characterized by the very low TiO<sub>2</sub> wt% in the Yezo Group  
523 were probably derived from such serpentine bodies that intruded in forearc  
524 region.

525           Moreover, Maruyama and Seno (1986) and Maruyama et al. (1997)  
526 indicate that the oceanic ridge that existed between the Izanagi-Kura Plate and  
527 the Pacific Plate was located around Japan arc in late Cretaceous time.  
528 Remarkable igneous activity related to the subduction of young and hot plate  
529 was reported around eastern Asia, i.e. eastern part of the North China (Ling et  
530 al., 2009; Zhang et al., 2011), Korean peninsula (Kim et al., 2005) and Japanese  
531 islands (Kinoshita, 1995, 2002; Hara and Kimura, 2008). Though the detail of  
532 paleogeography of the Japanese islands are still obscure, the subduction of  
533 young and hot plate widely affected to northern Japan, resulting the occurrence  
534 of adakitic activity of Lower Cretaceous granites and Lower Cretaceous to  
535 Eocene high-Mg andesite (Watanabe et al., 1993; Tsuchiya et al., 2005, 2007). In  
536 the Kitakami Massif, the Lower Cretaceous granites yield 110-121 Ma  
537 radiometric ages (Shibata et al., 1978) and the Lower Cretaceous volcanic rocks  
538 show 93(?) -121 Ma (Tsuchiya et al., 2005). The dike rocks, which were affected  
539 by thermal metamorphism by the Lower Cretaceous granites, were dated as  
540 117-134 Ma (Tsuchiya et al., 2005). The chromian spinels frequently occur in

541 high-Mg andesite and boninite as phenocrysts or inclusions in phenocrysts.  
542 Several spinels, showing higher Cr# and moderately low TiO<sub>2</sub> and very low TiO<sub>2</sub>,  
543 in the Kuji Group, could also be derived from high-Mg andesite, because the  
544 sandstones in the Kuji Group contain coarse-grained euhedral chromian spinels  
545 and the chemical composition of the spinels are overlapped to those of boninites  
546 from the Izu–Mariana forearc (Yajima and Fujimaki, 2001).

547         The direction and velocity of relative motion of oceanic plate with  
548 respect to the Eurasian plate was changed from northward to westward around  
549 80-90 Ma (Maruyama and Seno, 1986). The Kuji Group was contemporaneously  
550 deposited in Santonian-Campanian time when the northward motion of oceanic  
551 plate transited to westward. The transition of plate motion with a high  
552 convergence rate probably changed the forearc morphology. The morphological  
553 change could cause the transformation of sediment-supply and transport  
554 systems, including conversion of catchment area and transport direction, by  
555 uplift of forearc region and tectonic ridge in trench slope break, as reported from  
556 the Tonga forearc (Wright et al., 2000). Therefore there is a possibility that the  
557 provenance of the detrital chromian spinels changed from previous serpentine  
558 bodies infiltrated in forearc region to island arc type volcanic terrane as the  
559 Rebun-Kabato Belt. The very small amount of the low TiO<sub>2</sub> spinels in the  
560 sandstones of the Kuji Group implies the possibilities that a large amount of the  
561 detritus supplied from the volcanic terrane suppressed the derivation from

562 ultramafic rocks. Alternatively, the morphological transformation in forearc  
563 area might have modified previous sediment supply and transport systems  
564 completely.

565

## 566 **9. Implication for tectonics of the Asian continental margin during Cretaceous**

567 Lower Cretaceous island arc type volcanic rocks have been reported in  
568 the Harachiyama Formation in the North Kitakami Terrane and Rebun-Kabato  
569 Belt in Hokkaido island (Fig. 1-B; Segawa and Furuta, 1978; Sasaki and  
570 Tsuchiya, 1999; Okada and Sakai, 2000; Tsuchiya et al., 2005). Some of the  
571 volcanic rocks in the Rebun-Kabato Belt belong to both Berriasian and  
572 Cenomanian age (Nagata et al., 1986). Therefore, the Rebun-Kabato Belt is  
573 considered to be a magmatic belt along the eastern margin of the Asian  
574 continent extending south to the northern Japan arc that formed during the  
575 Cretaceous.

576 The characteristic volcanic activity similar to the Rebun-Kabato Belt is  
577 possibly recorded in the Cretaceous Terranes in Far East Russia and Sakhalin  
578 Island (Fig. 13). Cretaceous volcanic rocks exhibiting similar characteristics  
579 occur in Moneron Island, Far East Russia, which is located northwest of  
580 Hokkaido Island, Japan. This area is regarded as a northern extension of the  
581 Rebun-Kabato Belt (Simanenko et al., 2011). The Kamyshovy Terrane in  
582 Sakhalin Island, Far East Russia, located north of Hokkaido Island, Japan,

583 contains similar rock assemblages as those of Cretaceous island arc basalts and  
584 andesites with volcano-sedimentary rocks (Malinovsky et al., 2006). In the  
585 Sikhote Alin mountain range in Russia, similar rocks are present in the Kema  
586 Terrane, which is composed of Barremian(?)–Albian turbidites that contain  
587 siltstones, sandstones, conglomerates, tuff, and basaltic volcanic rocks  
588 (Malinovsky et al., 2006). These Cretaceous volcanic rocks were likely created  
589 by a series of volcanic arcs in the eastern margin of the Asian continent  
590 (Malinovsky et al., 2006).

591         Although the volcanic rocks formed in island arc settings constitute the  
592 chief provenance of the Kuji Group, even a small amount of the detritus  
593 supplied from high-Mg andesite possibly indicates a different tectonic episode.  
594 In this case, the chromian spinels that possibly came from high-Mg andesites  
595 are indicators of subduction of a very young and hot oceanic plate (Meijer, 1980).

596         The tectonic conditions of the Cretaceous magmatic arc, including the  
597 volcanic rocks of the Kamyshovy Terrane in Sakhalin Island and Kema Terrane  
598 in the Sikhote-Alin mountain range, are still obscure. The characteristics of  
599 volcanic activity, relative geographical location and tectonic setting of each  
600 terranes is also ambiguous before Paleogene period, because of post-Cretaceous  
601 tectonic disturbance, covering by Neogene-Paleogene deposits and major erosion  
602 with uplift. The information from detrital heavy mineral grains in the  
603 sedimentary rocks, as demonstrated in this study, contributes to reconstruction

604 of the temporal and special distributions of distinct igneous and tectonic  
605 activities. Those works reveal the tectonic development of the Cretaceous island  
606 arc in eastern Asian margin with probable tectonic episode of particular  
607 volcanic activity influenced by hot and young plate subduction.

608

## 609 **Conclusions**

610         The Upper Cretaceous Kuji Group, which formed in a small forearc  
611 basin on the Early Cretaceous volcanic belt in northern Japan, is mainly  
612 comprised of clastic sedimentary rocks deposited in fluvial and shallow marine  
613 environments.

614         Sandstone petrography revealed a provenance of a thermally  
615 metamorphosed Jurassic accretionary complex known as the North Kitakami  
616 Terrane and a Cretaceous volcanic belt known as the Rebun-Kabato Belt  
617 adjacent to the basin. The compositions of detrital garnets indicate origins of a  
618 sediment supply from the sandstone of the North Kitakami Terrane and contact  
619 aureoles of the Lower Cretaceous granites. Detrital tourmalines suggest an  
620 origin from meta-sedimentary rocks accompanied by granites and pegmatites.  
621 The composition of the detrital chromian spinels varies widely, indicating  
622 source lithologies such as tholeiitic and intra-oceanic plate basalts of the North  
623 Kitakami Terrane, and island arc basalt on the basis of Cr# and TiO<sub>2</sub> wt%.  
624 Many of the spinels derived from island arc volcanic rocks were perhaps derived

625 from high-Mg andesite. Therefore, these chromian spinels indicate a setting  
626 that includes volcanism with high-Mg andesite occurring in Early Cretaceous  
627 times.

628 In a comparison of chemical composition of the chromian spinels  
629 between Lower and Upper Cretaceous deposits in northern Japan, chromian  
630 spinels showing very low TiO<sub>2</sub> wt% prevailed in the Lower Cretaceous  
631 (Aptian-Albian), while chromian spinels showing moderately low TiO<sub>2</sub> wt%  
632 predominated in the Upper Cretaceous (Santonian-Campanian). This clear  
633 difference suggests the oceanic plate motion around the Japanese islands  
634 affected in the change of source rock assemblage in northern Japan in  
635 mid-Cretaceous time.

636 The Rebun-Kabato Belt in the northern Japan, the Cretaceous terranes  
637 in the Sikhote-Alin mountain range and Sakhalin Island in Russia, are believed  
638 to have created a Cretaceous magmatic arc in the Asian margin, although the  
639 nature of these arc has been poorly understood. We conclude that the  
640 characteristics of detrital heavy mineral composition in the Kuji Group give key  
641 evidence showing interaction between the swaying of young and hot plate and  
642 development of the Cretaceous arc formed in the eastern Asian margin.

643

#### 644 **Acknowledgements**

645 We acknowledge Mr. T. Tsugane and Prof. K. Makino for help for the

646 EDS analyses. We thank Prof. K. Hoyanagi, Dr. K. Ishida and Prof. S.  
647 Harayama for helpful comments. K. Hisada for suggestions on source rocks of  
648 detrital chromian spinels. We also thank Dr. M. Kawamura for suggestions on  
649 source rock of detrital garnets in the Northern Kitakami Terrane. We are  
650 grateful to Prof. S. Critelli and anonymous reviewer for their constructive  
651 comments and valuable suggestions that significantly improved the initial  
652 paper. We also thank to Dr. E. Koutsoukos for editorial handling.

653

#### 654 **References**

- 655 Ando, H., 2003. Stratigraphic correlation of Upper Cretaceous to Paleocene  
656 forearc basin sediments in Northeast Japan: cyclic sedimentation and basin  
657 evolution. *Journal of Asian Earth Sciences* 21, 921-935.
- 658 Arai, S., 1992. Chemistry of chromian spinel in volcanic rocks as a potential  
659 guide to magma chemistry. *Mineralogical Magazine* 56, 173–184.
- 660 Arai, S., Okada, H., 1991. Petrology of serpentine sandstone as a key to tectonic  
661 development of serpentine belts. *Tectonophysics* 195, 65–81.
- 662 Arthur, M.A., von Huene, R., Adelseck, C.G.Jr., 1980. 14. Sedimentary  
663 Evolution of the Japan Fore-Arc Region off Northern Honshu, Legs 56 and  
664 57, Deep Sea Drilling Project, in Initial Reports of the Deep Sea Drilling  
665 Project, 56, 57, 521-568.
- 666 Barnes, S.J., Roeder, P.L., 2001. The range of spinel compositions in terrestrial

667 mafic and ultramafic rocks. *Journal of Petrology* 42, 2279–2302.

668 Caracciolo, L., Critelli, S., Innocenti, F., Kolios, N., MANETTI P., 2011,  
669 Unraveling provenance from Eocene-Oligocene sandstones of the Thrace  
670 Basin, North-east Greece. *Sedimentology* 58, 1988-2011.

671 Chang, K., 1995. Aspects of geologic history of Korea. *Journal of the Geological*  
672 *Society of Korea* 31, 72–90.

673 Coleman, R.G., Lee, D.E., Beatty, L.B., Brannock, W.W., 1965. Eclogites and  
674 eclogites: their differences and similarities. *Geological Society of America*  
675 *Bulletin* 76, 483—508.

676 Critelli, S., Ingersoll, R.V., 1994. Sandstone petrology and provenance of the  
677 Siwalik Group (northwestern Pakistan and western-southeastern Nepal).  
678 *Journal of Sedimentary Research* A64, 815-823.

679 Critelli, S., Ingersoll, R.V., 1995. Interpretation of neovolcanic versus  
680 palaeovolcanic sand grains: an example from Miocene deep-marine  
681 sandstone of the Topanga Group (Southern California). *Sedimentology* 42,  
682 783-804.

683 Critelli, S., Marsaglia, K.M., Busby, C.J., 2002. Tectonic history of a Jurassic  
684 backarc basin sequence (the Gran Cañon Formation) based on compositional  
685 modes of tuffaceous deposits. *Geological Society of America Bulletin* 114,  
686 515-527.

687 Critelli, S., Le Pera, E., 1994. Detrital modes and provenance of Miocene

688 sandstones and modern sands of the southern Appennines thrust-top basins,  
689 Italy. *Journal of Sedimentary Research* A64, 824–835.

690 Deer, W.A., Howie, R.A., Zussman, J., 1992. An Introduction to the.  
691 Rock-Forming Minerals. Longman, Hong Kong, 696 pp.

692 Dick, H.J.B., Bullen, T., 1984. Chromian spinel as a petrogenetic indicator in  
693 abyssal and alpine-type peridotites and spatially associated lavas.  
694 *Contributions to Mineralogy and Petrology* 86, 54-76.

695 Dickinson, W.R., Suczek, C.A., 1979. Plate tectonics and sandstone composition.  
696 *American Association of Petroleum Geologists Bulletin* 63, 2164–82.

697 Dickinson, W.R., Valloni R., 1980. Plate setting and provenance of sands in  
698 modern basins. *Geology* 8, 82–86.

699 Dickinson, W.R., Bear L.S., Brakenridge G.R., Erjavec J.L., Ferguson R.C.,  
700 Inman K.F., Kepp R.A., Lindberg F.A. Ryberg P.T., 1983. Provenance of  
701 North American Phanerozoic sandstones in relation to tectonic setting.  
702 *Geological Society of America Bulletin* 94, 222–235.

703 Ehiro, M., Yamakita, S., Takahashi, S., Suzuki, N., 2008. Jurassic accretionary  
704 complexes of the North Kitakami belt in the Akka-Kuji area, Northeast  
705 Japan. *Journal of the Geological Society of Japan* 144, 121–139 (in Japanese,  
706 with English abstract).

707 Einaudi, M.T. and Burt, D.,M. 1982. Introduction; terminology, classification,  
708 and composition of skarn deposits. *Economic Geology* 77, 745-754.

709 Fujimaki, H., Yomogida, K., 1986a. Petrology of Hayachine ultramafic complex  
710 in contact aureole, NE Japan. I: primary and metamorphic minerals.  
711 Journal of Japan Association of Mineralogy, Petrology and Economic geology  
712 81, 1-11. (in Japanese, with English abstract)

713 Fujimaki, H., Yomogida, K., 1986b. Petrology of Hayachine ultramafic complex  
714 in contact aureole, NE Japan. II: Metamorphism and origin of the complex.  
715 Journal of Japan Association of Mineralogy, Petrology and Economic geology  
716 81, 59-66.

717 Hamano, K., Iwata, K., Kawamura, M., Kitakami Paleozoic Research Group,  
718 2002. Late Devonian conodont age of red chert intercalated in greenstones of  
719 the Hayachine Belt, Northeast Japan. Journal of the Geological Society of  
720 Japan 108, 114-122. (in Japanese, with English abstract)

721 Hanai, T., Obata, I., Hayami, I., 1968. Notes on the Cretaceous Miyako Group.  
722 Memoirs of the National Science Museum 1, 20-28 (in Japanese, with  
723 English abstract).

724 Hara, H. and Kimura, K., 2008. Metamorphic and cooling history of the  
725 Shimanto accretionary complex, Kyushu, Southwest Japan: Implications for  
726 the timing of out-of-sequence thrusting. Island Arc 17, 546-59.

727 Henry, D.J., Guidotti, C.V., 1985. Tourmaline as a petrogenetic indicator  
728 mineral: an example from the staurolite-grade metapelites of NW Maine.  
729 American Mineralogist 70, 1-15.

730 Hisada, K., Arai, S., Lee, Y.I., 1999, Tectonic implication of Lower Cretaceous  
731 chromian spinel-bearing sandstones in Japan and Korea. *Island Arc* 8,  
732 336-348.

733 Hisada, K., Takashima, S., Arai, S., Lee, Y.I., 2008. Early Cretaceous  
734 paleogeography of Korea and Southwest Japan inferred from occurrence of  
735 detrital chromian spinel. *Island Arc* 17, 471-484.

736 Inazuki, T. 1981. Two kinds of garnet amphibolites in the Momose-Mizunashi  
737 district, Hida metamorphic belt, central Japan. *Journal of the Faculty of*  
738 *Science, Hokkaido University, Series IV, Geology and Mineralogy* 20, 21-33.

739 Ingersoll, R.V., 1978. Petrofacies and petrology evolution of the Late Cretaceous  
740 fore-arc basin northern and central California. *Journal of Geology* 86,  
741 335-352.

742 Japan Natural Gas Association and Japan Offshore Petroleum Development  
743 Association, 1992. *Recent oil exploration in Japan (revised edition)*, 520 p.,  
744 Tokyo, Japan (in Japanese).

745 Kamenetsky, V.S., Crawford, A.J., Meffre, S., 2001. Factors controlling  
746 chemistry of magmatic spinel; an empirical study of associated olivine,  
747 Cr-spinel and melt inclusions from primitive rocks. *Journal of Petrology* 42,  
748 655-671.

749 Kato, M., Fujiwara, Y., Minoura, N., Koshimizu, S., Saito, M., 1986. Fission  
750 track age of zircons in the Upper Cretaceous Yokomichi Formation, Northern

751 Kitakami Mountains, Japan. *Journal of the Geological Society of Japan* 92,  
752 821-822.

753 Kawamura, M., Kato, M., Kitakami Paleozoic Research Group, 1990. Southern  
754 Kitakami Terrane. In Ichikawa, K., Mizutani, S., Hara, I., Hada S. and Yao A.  
755 eds., *Pre-Cretaceous Terranes of Japan*, Publication of IGCP Project No.224,  
756 Osaka, pp. 249-266.

757 Kawamura, M., Uchino, T., Gouzu, C., Hyodo, H., 2007. 380 Ma  $^{40}\text{Ar}/^{39}\text{Ar}$  ages  
758 of the high-P/T schists obtained from the Nedamo Terrane, Northeast Japan.  
759 *Journal of the Geological Society of Japan* 113, 492-499.

760 Kawano, Y., Ueda, Y., 1967. Periods of the igneous activities of the granitic rocks  
761 in Japan by K-A dating method. *Tectonophysics* 4, 523-530.

762 Kim SW, Oh CW, Choi SG, Ryu IC, Itaya T., 2005. Ridge subduction-related  
763 Jurassic plutonism in and around the Okcheon metamorphic belt, South  
764 Korea, and implications for Northeast Asian tectonics. *International*  
765 *Geological Review* 47, 248–269.

766 Kiminami, K., Komatsu, M., Niida, K., Kito, N., 1986. Tectonic divisions and  
767 stratigraphy of the Mesozoic rocks of Hokkaido, Japan. In: Editorial  
768 committee of geology and tectonics of Hokkaido (Eds.), *Geology and Tectonics*  
769 *of Hokkaido*. Monograph of the Association for the Geological Collaboration  
770 in Japan 31, pp. 1-15 (in Japanese, with English Abstract).

771 Kimura, G., 1994. The latest Cretaceous-early Paleogene rapid growth of

772 accretionary complex and exhumation of high pressure series metamorphic  
773 rocks in northwestern Pacific margin. *Journal of the Geophysical Research*  
774 99, 22147–22164.

775 Kimura, Y., Aizawa, J., Sasaki, K., 2005. Sedimentary environments and  
776 diagenetic ranks of the amber-bearing strata distributed around the Kuji  
777 area, Iwate Prefecture, northeast Japan. *Fukuoka University Science*  
778 *Reports* 35, 31-40. (in Japanese, with English abstract)

779 Kinoshita, O., 1995. Migration of igneous activities related to ridge subduction  
780 in Southwest Japan and the East Asian continental margin from the  
781 Mesozoic to the Paleogene. *Tectonophysics* 245, 25–35.

782 Kinoshita, O., 2002. Possible manifestations of slab window magmatisms in  
783 Cretaceous southwest Japan. *Tectonophysics* 344, 1–13.

784 Kondo, H., 1993. Igneous rocks of the Kumaneshiri Group in the Kabato  
785 Mountains, Hokkaido, Japan - Characterization of the alkali rich igneous  
786 rocks in the Cretaceous volcanic zone of Northeast Japan-. *Journal of the*  
787 *Geological Society of Japan* 99, 347-364. (in Japanese, with English abstract)

788 Ling M, Wang F, Ding X, Hu, Y.H, 2009. Cretaceous ridge subduction along the  
789 Lower Yangtze River Belt, eastern China. *Economic Geology* 104, 303–321.

790 Lithgow-Bertelloni, C., Richards, M. A., 1998. The Dynamics of Cenozoic and  
791 Mesozoic Plate Motions. *Reviews of Geophysics* 36, 27–78.

792 Malinovsky, A., Golozoubov, V., Simanenko, V. P., 2006. The Kema Island-Arc

793 Terrane, Eastern Sikhote Alin: Formation Settings and Geodynamics.  
794 Doklady Earth Science 410, 1026-1029.

795 Maruyama, S., Seno, T., 1986. Orogeny and relative plate motion: Example of  
796 the Japanese islands. Tectonophysics 127, 305–329.

797 Maruyama, S., Isozaki, Y., Kimura, Y., Terabayashi, M., 1997. Paleogeographic  
798 maps of the Japanese islands: Plate tectonic synthesis from 750 Ma to the  
799 present. Island Arc 6, 121–42.

800 Matsumoto, T., Obata, I., Tashiro, M., Ohta, Y., Tamura, M., Matsukawa, M.  
801 Tanaka, H., 1982. Correlation of marine and non-marine formations in the  
802 Cretaceous of Japan. Fossils 31, 1-26 (in Japanese, with English abstract).

803 Meijer, A., 1980. Primitive arc volcanism and a boninite series: Examples from  
804 western Pacific island arcs. In: Hayes, D. E. (Eds.), The Tectonic and  
805 Geologic Evolution of Southeast Asian Seas and Islands, American  
806 Geophysics Union Monograph 23, pp. 269–282.

807 Miki, A., 1977. Late Cretaceous pollen and spore floras of northern Japan:  
808 composition and interpretation. Journal of the Faculty of Science, Hokkaido  
809 University, Series IV, 17, 399-436.

810 Minoura, K., 1990. The Pre-Cretaceous geology and tectonics of northern  
811 Kitakami region. In: Ichikawa, K., Mizutani, S., Hara, I., Hada, S., Yao, A.  
812 (Eds.), Pre-Cretaceous Terranes of Japan. Publication of IGCP Project No.  
813 224: Pre-Jurassic Evolution of Eastern Asia. Osaka, pp. 267–279.

814 Miura, R., Ishiwatari, A., 2001. Petrology of the oceanic island tholeiite-origin  
815 greenstones in the Shimamori Formation, North Kitakami belt,  
816 northeastern Japan. *Japanese Magazine of Mineralogical and Petrological*  
817 *Sciences* 30, 1-16 (in Japanese, with English abstract).

818 Miyashiro, A., 1953. Calcium-poor garnet in relation to metamorphism.  
819 *Geochimica et Cosmochimica Acta* 4, 179-208.

820 Morton, A.C., 1985. Heavy minerals in provenance studies. In: Zuffa, G.G. (Ed.),  
821 *Provenance of Arenites*. Reidel, Dordrecht, pp. 249–277.

822 Morton, A.C., Hallsworth, C.R., 1999. Processes controlling the composition of  
823 heavy mineral assemblages in sandstones. *Sedimentary Geology* 124, 3–29.

824 Nagahama, H., Terui, K., 1977. Composition of sandstones and conglomerates  
825 in the Kuji and Noda Group. Abstract of 84th annual Meeting of Geological  
826 Society of Japan, 148 (in Japanese).

827 Nagata, M., Kito, N., Niida, K., 1986. The Kumaneshiri Grop in the Kabato  
828 Mountais: the age and nature as an Early Cretaceous volcanic arc. In:  
829 Editorial committee of geology and tectonics of Hokkaido (Eds.), *Geology and*  
830 *Tectonics of Hokkaido*. Monograph of the Association for the Geological  
831 *Collaboration in Japan* 31, pp. 63-79. (in Japanese, with English abstract)

832 Nakamoto, K., Yasuda, N., Kawamura, M., 1996. Chemical composition and  
833 origin of the detrital garnet in the Mesozoic accretionary complex, Oshima  
834 Belt and North Kitakami Belt, northeast Japan. Abstract of 100th annual

835 meeting of Geological Society of Japan, 375 (in Japanese).

836 Nanayama, F., 1997, Stratigraphic occurrence of detrital chromian spinels from  
837 the Yezo forearc basin, and its bearing on the emplacement age of the  
838 Kamuikotan ultrabasic rocks, central Hokkaido, northeast Japan. *Journal of*  
839 *the Geological Society of Japan*, 103, 97-112. (in Japanese with English  
840 abstract)

841 Nanayama, F, Nakagawa, M., Kito, N. and Kato, T., 1997. New evidence and  
842 preliminary report for the age of intrusion of the Kamuikotan ultramafic  
843 rocks: discovery of detrital chromian spinels from the Lower Yezo Group, in  
844 the Sorachi-Yezo Belt, central Hokkaido, Japan and their significance.  
845 Commemorative volume for Professor M. Kato, 175-182. (in Japanese with  
846 English abstract)

847 Okada, H., Sakai, T., 2000. The Cretaceous System of the Japanese Islands and  
848 its physical environments. In Okada, H., Mather, N. J. (Eds.), *Cretaceous*  
849 *Environments of Asia*, Elsevier, Amsterdam, pp. 113-144.

850 Okami, K., Ehiro, M., 1988. Review and recent progress of studies on the  
851 pre-Miyakoan sedimentary rocks of the northern Kitakami massif,  
852 Northeast Japan. *Earth Science (Chikyu Kagaku)* 42, 187-201 (in Japanese,  
853 with English abstract).

854 Okami, K., Ehiro, M., Koshiya, S., 1994. Compositional changes of the  
855 sandstone in relation to evolution of a mobile belt - an example of the

856 Paleozoic to Mesozoic sandstones of North Japan. In Kumon F., Yu  
857 K.M.(Eds.), Proceedings of the 29th International Geological Congress;  
858 Sandstone petrology in relation to Tectonics, VSP International Sciences  
859 Publishers, Utrecht, The Netherlands, pp. 119-134.

860 Osawa, M., Nakanishi, S., Tanahashi, M., Oda, H., 2002. Journal of the  
861 Japanese association for petroleum technology 67, 38-51. (in Japanese, with  
862 English abstract)

863 Saito, Y., Hashimoto, M., 1982. South Kitakami Region: an allochthonous  
864 terrane in Japan. Journal of Geophysical Research 87 (b), 3691–3696.

865 Sasaki, K., Tsuchiya, N., 1999. Stratigraphy and volcanic history of Early  
866 Cretaceous volcanic rocks in Hachinohe-Tanesashi area, northern Kitakami  
867 Mountains, Japan. Abstract of 106th annual meeting of the Geological  
868 Society of Japan 106, 254.

869 Segawa, J., Furuta, T., 1978. Geophysical stud of the mafic belts along the  
870 margins of the Japanese islands. Tectonophysics 44, 1-26.

871 Simanenko, V.P., Rasskazov, S.V., Yasnygina, T.A., Simanenko, L.F., Chashchin,  
872 A. A., 2011. Cretaceous complexes of the frontal zone of the  
873 Moneron-Samarga Island arc: Geochemical data on the basalts from the  
874 deep borehole on Moneron Island, the Sea of Japan. Russian Journal of  
875 Pacific Geology 5, 26-46.

876 Shibata, K., Matsumoto, T., Yanagi, T., Hamamoto, R., 1978. Isotopic Ages and

877 Stratigraphic Control of Mesozoic Igneous Rocks in Japan. American  
878 Association of Petroleum Geologist Special Volume, Contributions to the  
879 Geologic Time Scale, 143 – 164.

880 Shimazu, M., 1979. Some problems on the Cretaceous-Paleogene igneous  
881 activity in the Kitakami Mountains. Memoir of the Geological Society of  
882 Japan 17, pp. 113-120 (in Japanese, with English abstract).

883 Shimazu, M., Teraoka, Y., 1962. Geology of Rikuchu-Noda, scale 1:50,000.  
884 Geological Survey of Japan, 53 (in Japanese, with English abstract).

885 Taira, A. and Tashiro, M., 1987. Late Paleozoic and Mesozoic accretion tectonics  
886 in Japan. Terra. Sci. Pub. Com., 1-45, Tokyo.

887 Takahashi, M., 1983. Space-time distribution of Late Mesozoic to Early  
888 Cenozoic magmatism in East Asia and its tectonic implications. In  
889 Hashimoto M., Uyeda S. (Eds.), Accretion Tectonics in the Circum-Pacific  
890 Regions, Terra Science Publication, Tokyo, pp. 69–88.

891 Taki, S., Iba, Y., Hikida, Y. and Yoshida, K., 2011, Lithostratigraphy of the  
892 Cretaceous in the upper reaches of the Chirashinai River, Teshionakagawa  
893 area, northern Hokkaido, Japan. Journal of the Faculty of Science, Shinshu  
894 University, 1-42. (in Japanese, with English abstract)

895 Takigami, Y., 1991.  $^{40}\text{Ar}$ – $^{39}\text{Ar}$  ages of igneous rocks near Miyako-City, Northeast  
896 Japan. Research Bulletin of Kanto Gakuen University 18, 105–114.

897 Terui, K., Nagahama, H., 1995. Depositional facies and sequences of the Upper

898 Cretaceous Kuji Group, Northeast Japan. Memoir of Geological Society of  
899 Japan 45, 238-249. (in Japanese, with English abstract)

900 Tsuchiya, N., Kimura, J., Kagami, H., 2007. Petrogenesis of Early Cretaceous  
901 adakitic granites from the Kitakami Mountains, Japan. Journal of  
902 Volcanology and Geothermal Research 167, 134-159.

903 Tsuchiya, N., Suzuki, S., Kimura, J., Kagami, H., 2005. Evidence for slab  
904 melt/mantle reaction: petrogenesis of Early Cretaceous and Eocene high-Mg  
905 andesites from the Kitakami Mountains, Japan. Lithos 79, 179-206.

906 Uchino, T., Kurihara, T., Kawamura, M., 2005. Early Carboniferous  
907 radiolarians discovered from the Hayachine Terrane, Northeast Japan: the  
908 oldest fossil age for clastic rocks of accretionary complex in Japan. Journal of  
909 the Geological Society of Japan 111, 249-252.

910 von Eynatten, H., 2003. Petrography and chemistry of sandstones from the  
911 Swiss Molasse Basin: an archive of the Oligocene to Miocene evolution of the  
912 Central Alps. Sedimentology 50, 703-724.

913 Watanabe, T., Buslov, M.M. and Koitabashi S., 1993. Comparison of arc-trench  
914 systems in the Early Paleozoic Gorny Altai and the Mesozoic-Cenozoic of  
915 Japan. In: Coleman R. G. (Ed.), Proceedings of the 29th International  
916 Geological Congress; Reconstructions of the Paleo-Asian ocean, VSP  
917 International Sciences Publishers, Utrecht, The Netherlands, pp. 160-177.

918 Wright, D.J., Bloomer, S.H., MacLeod, C.J., Taylor, B., Goodlife, A.M., 2000.

919 Bathymetry of the Tonga Trench and Forearc: a map series. *Marine*  
920 *Geophysical Researches* Volume 21, 489-512.

921 Yamaguchi, Y., Tsushima, H., Kitamura, N., 1979. Geologic Development of the  
922 Southern Part of "Taro Belt" and "Iwaizumi Belt" in the Kitakami Massif,  
923 Northeast Japan. *Contributions from the Institute of Geology and*  
924 *Paleontology Tohoku University* 80, 99-117. (in Japanese, with English  
925 abstract).

926 Yajima, K., Fujimaki, H., 2001. High-Ca and low-Ca boninites from Chichijima,  
927 Bonin (Ogasawara) archipelago: *Japanese Magazine of Mineralogical and*  
928 *Petrological Sciences* 30, 217-236.

929 Yoshida, K., Machiyama, H., 2004. Provenance of Permian sandstones, South  
930 Kitakami Terrane, Northeast Japan: implications for Permian arc evolution.  
931 *Sedimentary Geology* 166, 185-207.

932 Yoshida, K., Taki, S., Iba, Y., Sugawara, M., Hikida, Y., 2003. Discovery of  
933 serpentinite bearing conglomerate in the Lower Yezo Group, Hokkaido,  
934 northern Japan and its tectonic significance. *Journal of the Geological*  
935 *Society of Japan* 109, 336-344. (in Japanese, with English abstract)

936 Yoshida, K., Iba, Y., Taki, S., Sugawara, M., Tsugane, T., Hikida, Y., 2010.  
937 Deposition of serpentine-bearing conglomerate and its implications for Early  
938 Cretaceous tectonics in northern Japan. *Sedimentary Geology* 232, 1-14.

939 Zhang, C., Ma, C.O, Liao, Q.A., Zhang, J.Y., She, Z.B, 2011. Implications of

940 subduction and subduction zone migration of the Paleo-Pacific Plate beneath  
941 eastern North China, based on distribution, geochronology, and  
942 geochemistry of Late Mesozoic volcanic rocks. International Journal of Earth  
943 Science (Geol Rundsch) 100, 1665-1684.

944

945

946 **Figure and table captions**

947

948 Figure 1. A: Index map of study area. B: Distribution of Cretaceous volcanic  
949 rocks and division of geological belt compiled from Segawa and Furuta  
950 (1978) and Kiminami et al. (1986). C: division of the geological belts in the  
951 Kitakami Massif. The simplified geology is compiled from Kawamura et al.  
952 (1990), Tsuchiya et al. (2005), and Uchino et al. (2005).

953 Figure 2. Simplified geological map in the Noda area after Terui and Nagahama  
954 (1995).

955 Figure 3. Stratigraphy and age of the Kuji and Noda Group after Shimazu and  
956 Teraoka (1962). Stratigraphic markers after \*1: Shibata et al. (1978), \*2:  
957 Terui and Nagahama (1995), \*3: Kato et al. (1986) , \*4: Shimazu and  
958 Teraoka (1962).

959 Figure 4. Stratigraphic column and sampling horizons for sandstone petrology  
960 and chemistry of heavy mineral. The examined analyses are shown as (g)  
961 chemistry of detrital garnet, (c) chemistry of detrital chromian spinel, (t)  
962 chemistry of detrital tourmaline, (M) sandstone modal composition. mdst:  
963 mudstone, vfs.: very fine grained sandstone, fs.: fine-grained sandstone, cs.:  
964 coarse-grained sandstone, vcs.: very coarse grained sandstone, cg:  
965 conglomerate.

966 Figure 5. A: QmFLt and B: QFL triangular diagrams for the framework modes

967 of the sandstones, showing the different provenance fields defined by  
968 Dickinson et al. (1983). Abbreviations as in Table 1. Qm: monocrystalline  
969 quartz grains, F: feldspar grains, Lt: total lithic fragments, Q:  
970 monocrystalline quartz + chert grains, L: Lt-chert grains.

971 Figure 6. Photomicrographs of the sandstone in the Kunitan Formation (A)  
972 and Tamagawa Formation (B); Photomicrograph of the garnet grain (C),  
973 brown tourmaline grain (D), euhedral chromian spinel grains (E and F), in  
974 the Kunitan Formation, Kuji Group. All photomicrographs are taken under  
975 plane polarized light. Abbreviations for dominant rock fragments in (A) and  
976 (B); r: rhyolitic volcanic fragments; an: andesitic volcanic fragments; v:  
977 vitric volcanic fragments; ch: chert fragments; gr: granitic fragments.

978 Figure 7. Detrital garnet compositions. Pyrope - almandine - grossular +  
979 andradite + spessartine diagram. The shaded area indicates detrital garnet  
980 grains from sandstone in the North Kitakami Terrane (Nakamoto et al.,  
981 1996).

982 Figure 8. Detrital tourmaline compositions on Al-Fe-Mg and Ca-Fe-Mg  
983 diagrams. Discrimination fields for various rock types according to Henry  
984 and Guidotti (1985) are as follows: (a) Li-rich granitoids, pegmatites, and  
985 aplites; (b) Li-poor granitoids, pegmatites, and aplites; (c) hydrothermally  
986 altered granitic rocks; (d) aluminous pelrites and psammites; (e) Al-poor  
987 pelrites and psammites; (f) Fe<sup>3+</sup>-rich quartz-tourmaline rocks; (g) Low-Ca

988 meta-ultramafics; (h) metacarbonates and metapyroxenites; (1) Li-rich  
989 granitoids, pegmatites, and aplites; (2) Li-poor granitoids, pegmatites, and  
990 aplites; (3) Ca-rich pellites, psammites, and calc-silicates; (4) Ca-poor  
991 pellites, psammites, and quartz-tourmaline rocks; (5) metacarbonates; (6)  
992 meta-ultramafic rocks.

993 Figure 9. Detrital chromian spinel compositions of the Kuji Group. A: Mg#-Cr#  
994 diagram, Cb; Chichijima boninites after Yajima and Fujimaki (2001), Ib;  
995 island arc tholeiites and boninites after Kamenetsky et al. (2001), B: Cr#  
996 -TiO<sub>2</sub> wt% diagram, compositional fields are after Arai (1992). The shaded  
997 areas show the composition of oceanic-island tholeiites (greenstones) in the  
998 North Kitakami Terrane (Miura and Ishiwatari, 2001). C: TiO<sub>2</sub> wt%Al<sub>2</sub>O<sub>3</sub>  
999 wt% diagram, compositional fields are after Kamenetsky et al. (2001).  
1000 MORB; mid-ocean ridge basalt, OIB; ocean-island basalt, LIP; large  
1001 igneous province, ARC; island-arc magmas, SSZ; supra-subduction zone. D:  
1002 Fe<sup>3+</sup> - Cr - Al triangular diagram. Compositional fields are after Barnes and  
1003 Roeder (2001).

1004 Figure 10. Simplified stratigraphic scheme of the Kitakami Massif. N.K.T.:  
1005 North Kitakami Terrane, S.K.T.: South Kitakami Terrane.

1006 Figure 11. Schematic illustration of provenance and basin with tectonic  
1007 environments during the deposition of the Kuji Group. No scale implied.

1008 Figure 12. Figure showing the relationship between ocean plate motion

1009 (Maruyama and Seno, 1986) and stratigraphic change of TiO<sub>2</sub> content (wt%)  
1010 in detrital chromian spinels. The chemistry of chromian spinels in the Yezo  
1011 Group (Kamiji Formation) is after Yoshida et al. (2003). Occurrence of  
1012 detrital chromian spinels in the Yezo Group is based on Nanayama (1997),  
1013 Nanayama et al. (1997) and Yoshida et al. (2003, 2010). Pl: Paleocene; Sd:  
1014 Selandian.

1015 Figure 13. Schematic map showing the Mesozoic terranes in northern Japanese  
1016 islands and Shkhote Alin areas (modified from Simanenko et al., 2011). Sm:  
1017 Samarka, KM: Kiselevka–Manoma, Tkh: Taukhe, Ke: Kema, WS: Western  
1018 Sakhalin, N: Nabil, T: Terpeniya, Ka: Kamyshovy, S: Susunai, Mr: Marei, Oz:  
1019 Ozerskii, Ta: Tonin–Aniva, ON: Oshima-North Kitakami, RK: Rebun-Kabato,  
1020 SY: Sorachi–Yezo, K: Kamuikotan, I: Idonappu, H: Hidaka, Tk: Tokoro, Nm:  
1021 Nemuro.

1022

1023 Table 1. Modal composition of the sandstones in the Kuji Group. Qm:  
1024 monocrystalline quartz, Qp: polycrystalline quartz, Pl: plagioclase, Kf: k-feldspar,  
1025 Lvf: felsic volcanics, Lvb: intermediate-basic volcanics, Ls: sedimentary lithics, Lm:  
1026 metamorphic lithics, HM: heavy minerals. F: feldspar grains, Lt: total lithic  
1027 fragments, Q: monocrystalline quartz + chert grains, L: Lt-chert grains.

1028 Table 2. Chemical composition of detrital garnet grains from the sandstones in  
1029 the Kuji Group. Alm: almandine, Py: pyrope, Sp: spessartine, Gro: grossular,

1030 An: andradite.

1031 Table 3. Chemical composition of detrital tourmaline grains from the  
1032 sandstones in the Kuji Group.

1033 Table 4. Chemical composition of detrital chromian spinels from the sandstones  
1034 in the Kuji Group.

1035

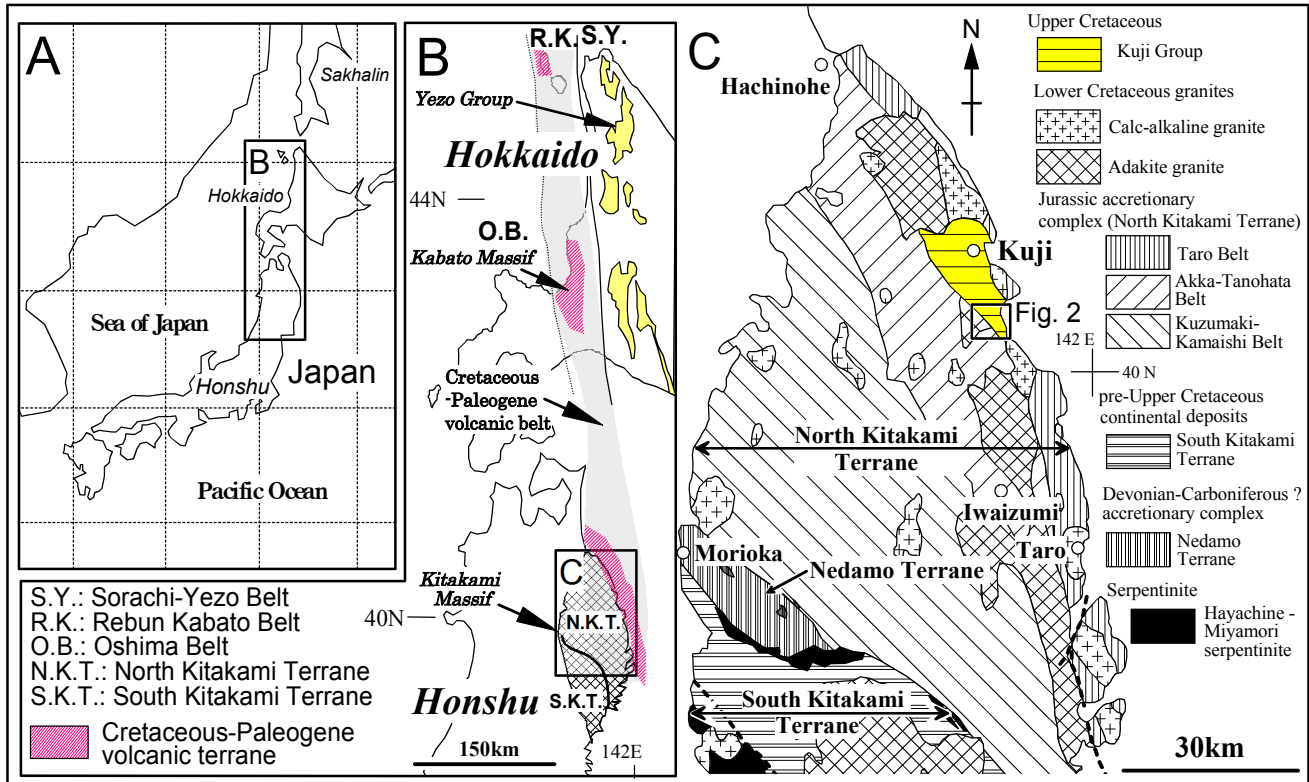


Fig.1 Nishio and Yoshida

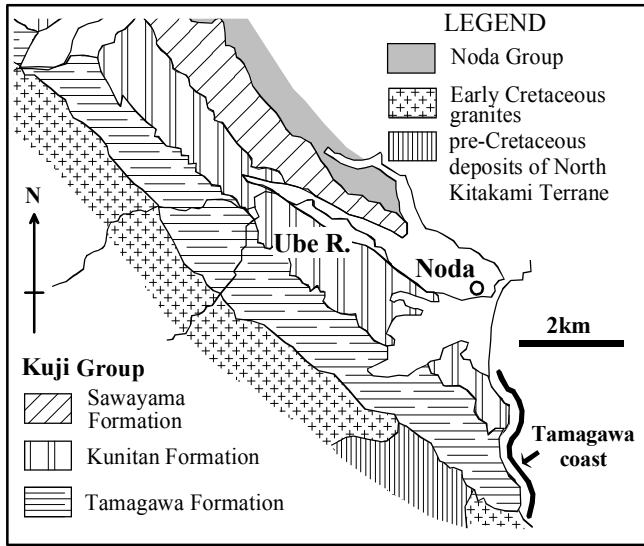


Fig. 2 Nishio & Yoshida

Age		Stratigraphy		
Paleogene		Noda Group	Kuki Formation	<i>Osmunda macrophylla</i> *4 <i>Taxodium dubium</i> *4
			Minato Formation	
Late Cretaceous	Early Campanian	Kuji Group	Sawayama Formation	71.2 ± 14.4Ma (fission track*3)
	Santonian		Kunitan Formation	<i>Inoceramus naumanni</i> *2 <i>Inoceramus japonicus</i> *2
	Coniacian		Tamagawa Formation	
Pre-Late Cretaceous		Tanohata Granite	Deposits of N.K.T.	110-121 Ma (granite, *1)

Fig.3 Nishio and Yoshida

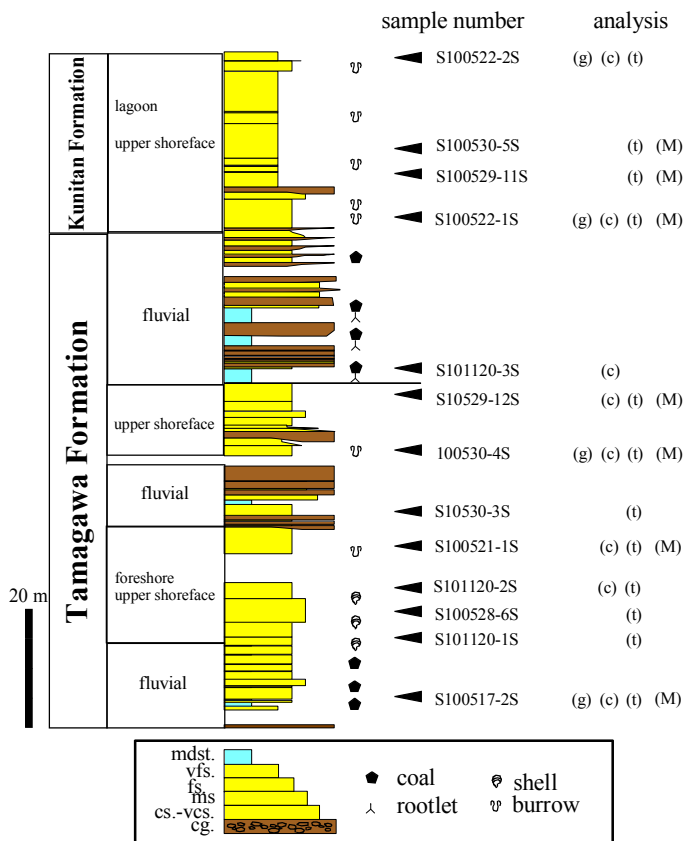


Fig.4 Nishio and Yoshida

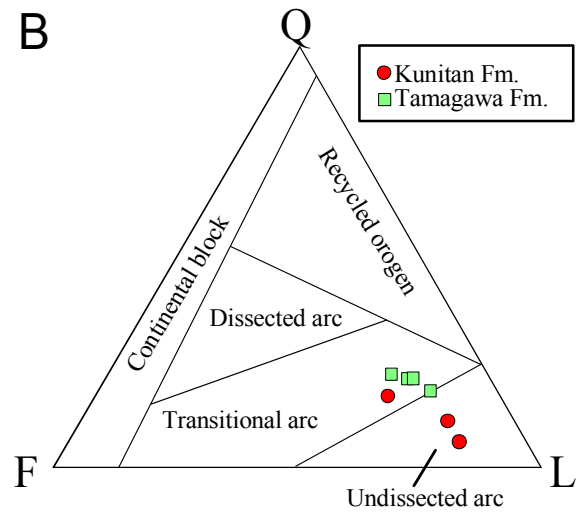
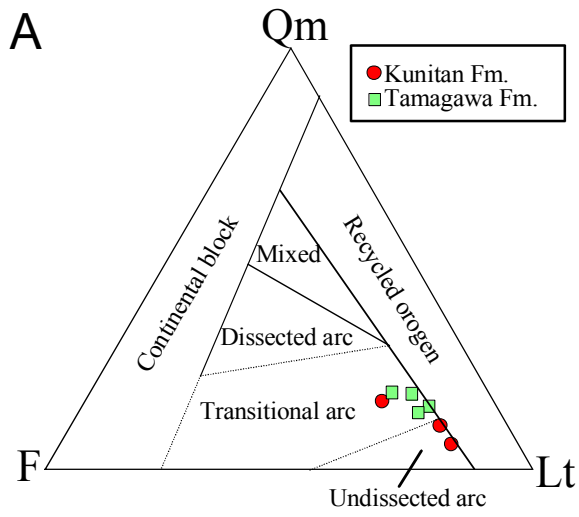


Fig.5 Nishio and Yoshida

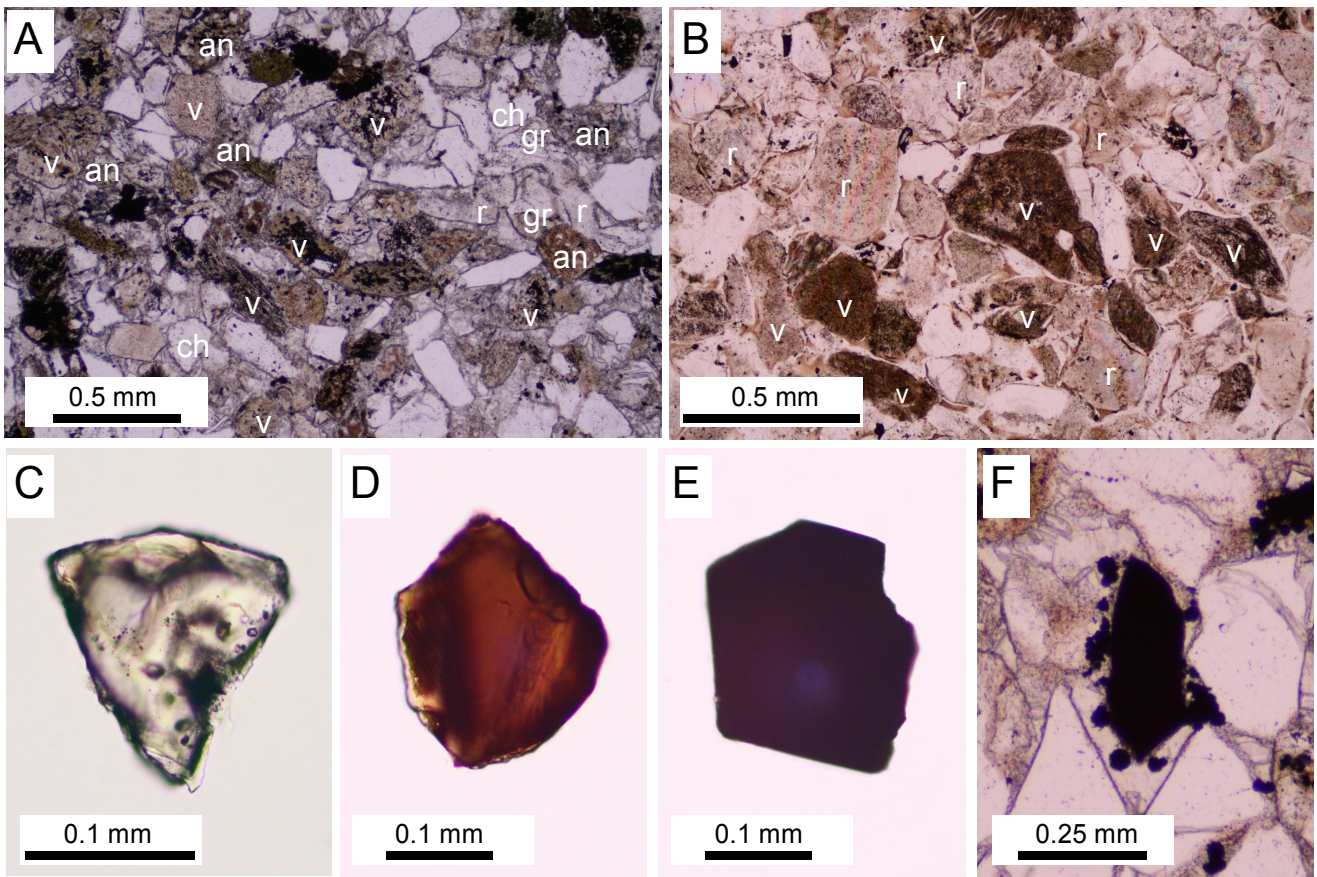


Fig.6 Nishio and Yoshida

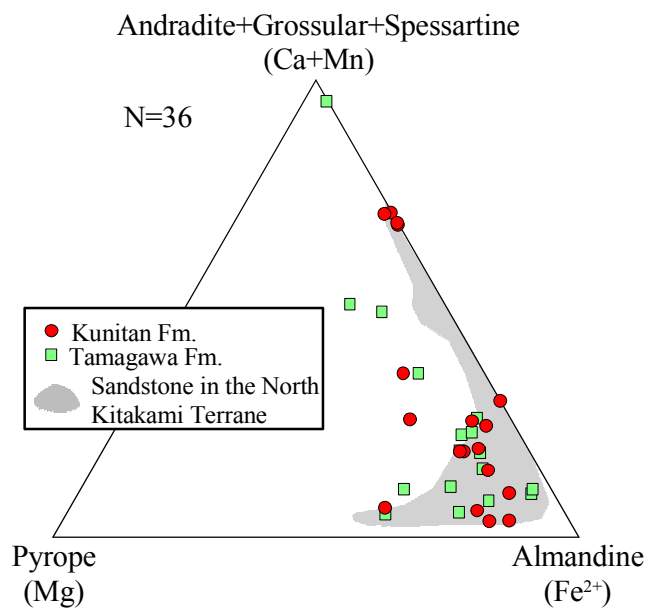


Fig.7 Nishio and Yoshida

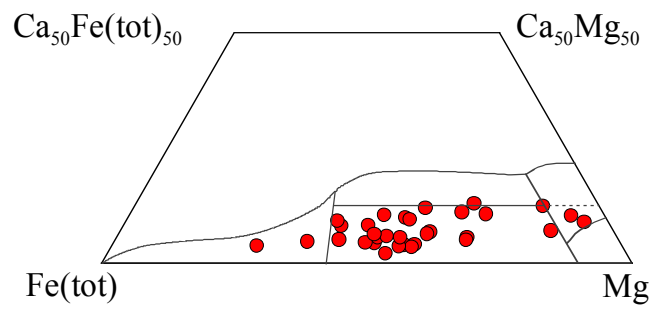
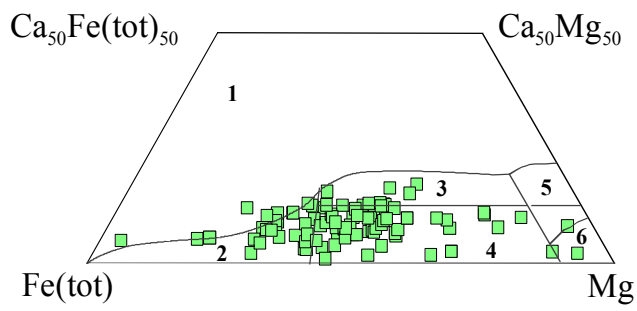
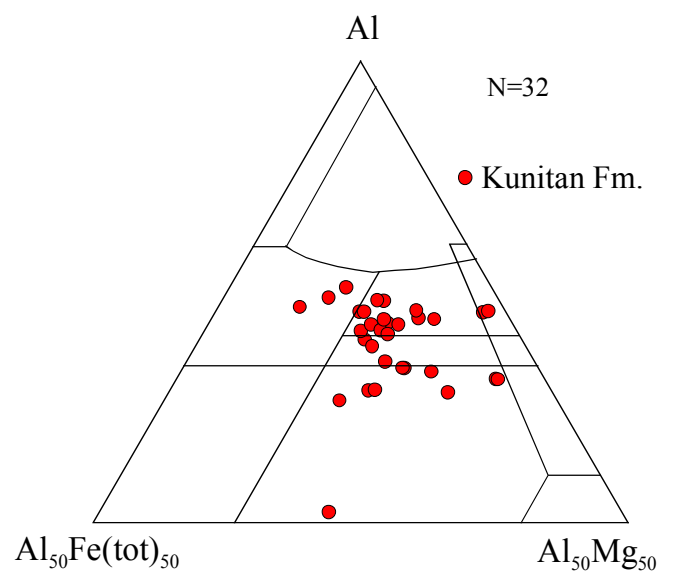
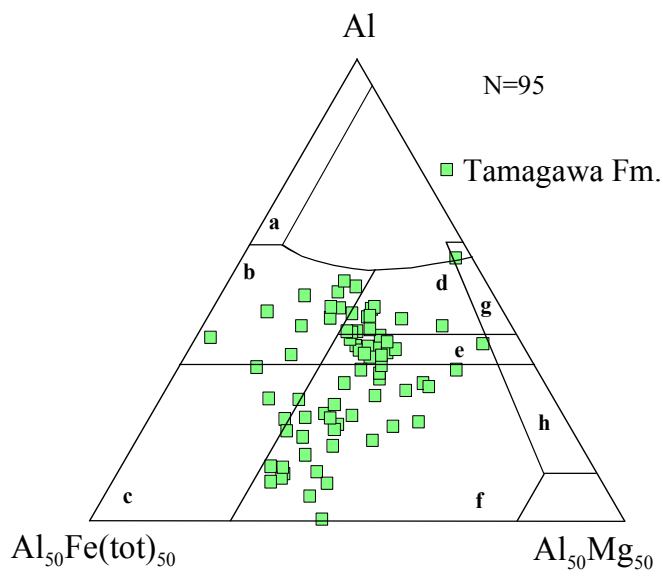


Fig.8 Nishio and Yoshida

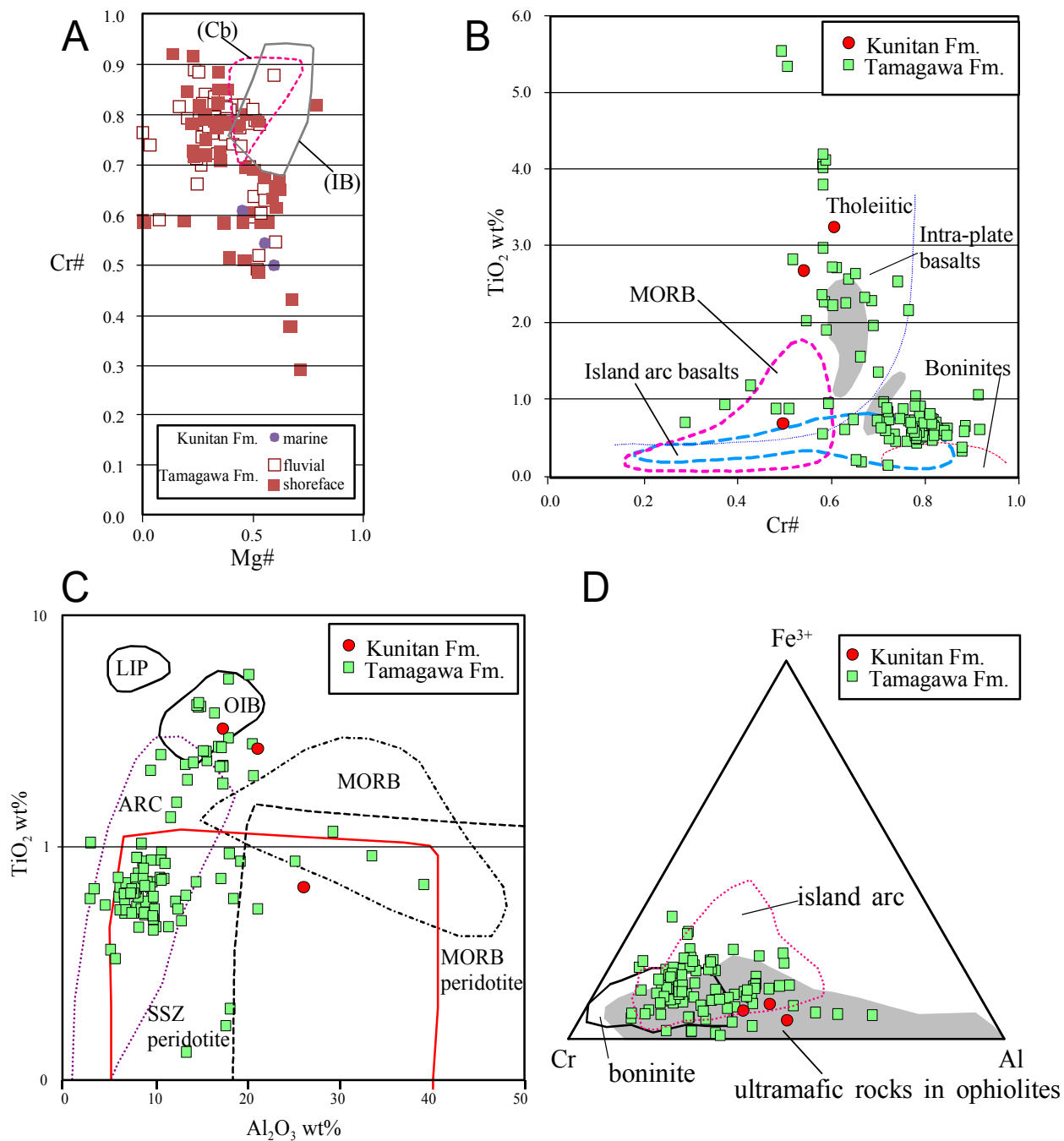


Fig.9 Nishio and Yoshida

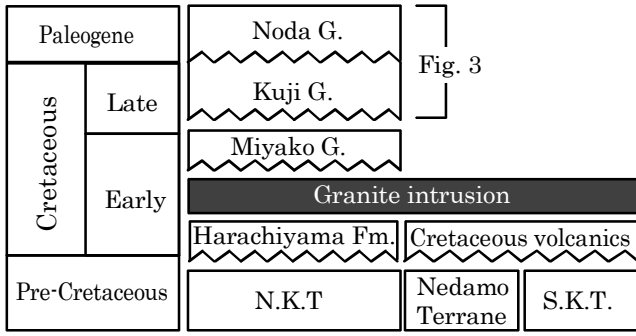


Fig.10 Nishio and Yoshida

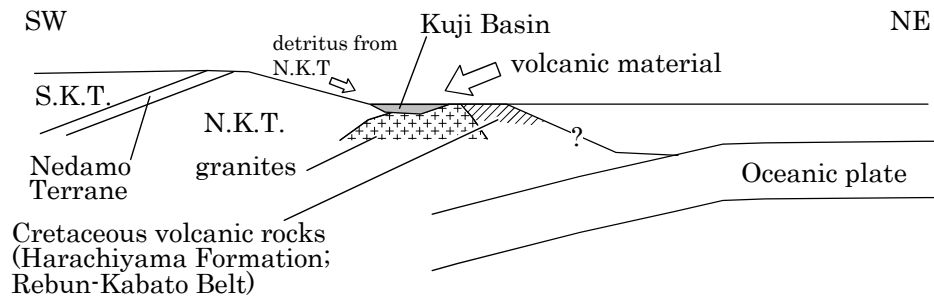


Fig.11 Nishio and Yoshida

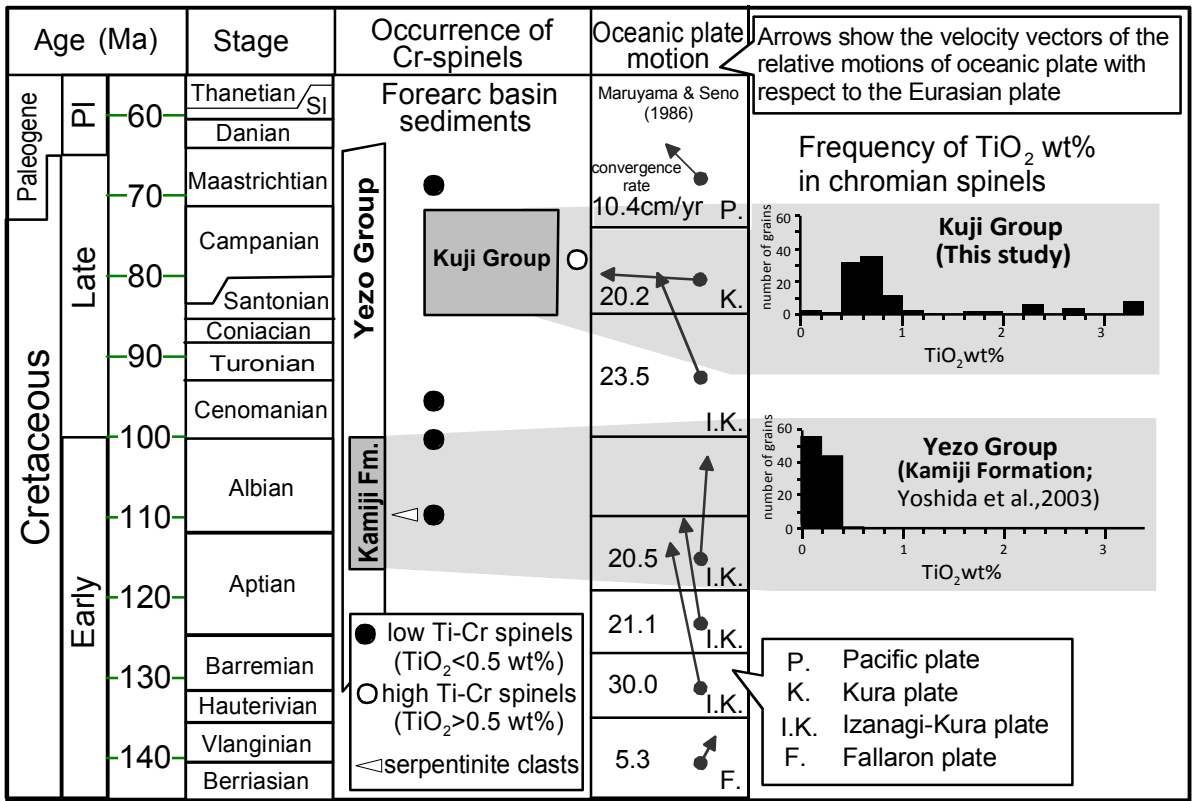


Fig.12 Nishio and Yoshida

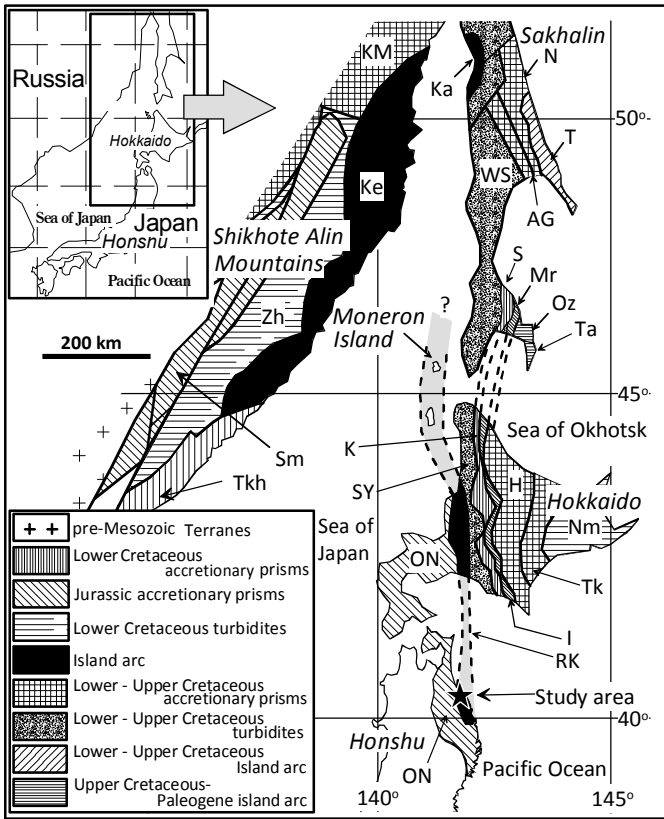


Fig.13 Nishio and Yoshida

Table 1 Modal composition of the sandstones in the Kuji Group.

Formation	Tm	Tm	Tm	Tm	Kn	Kn	Kn
Sample number	s100529-12s	s100530-4s	s100521-1s	s100517-2s	s100530-5s	s1005529-11s	s100522-1s
Qm	126	157	108	136	102	60	152
Qp	4	8	18	4	0	0	8
Pl	103	133	126	136	133	135	203
Kf	18	4	6	12	0	0	16
Lvf	575	542	480	426	723	796	560
Lvb	8	3	11	2	2	3	14
Ls	0	0	0	0	0	0	0
Lm	0	0	0	4	4	0	0
Chert	27	12	42	20	0	0	8
Cement	121	122	132	260	4	0	16
Matrix	9	0	6	0	12	4	0
Heavy Minerals	9	21	72	0	20	4	24
total	991	981	929	1000	980	998	977
flameword grain	861	859	791	740	964	994	961
Qm/QFLt	0.15	0.18	0.14	0.18	0.11	0.06	0.16
F/QFLt	0.14	0.16	0.17	0.20	0.14	0.14	0.23
Lt/QmFLt	0.71	0.66	0.70	0.62	0.76	0.80	0.61
Q/QFL	0.18	0.21	0.21	0.22	0.11	0.06	0.17
F/QFL	0.14	0.16	0.17	0.20	0.14	0.14	0.23
L/QFL	0.68	0.63	0.62	0.58	0.76	0.80	0.60

Tm: Tamagawa Formation, Kn: Kunitan Formation

Table 2 Chemical composition of detrital garnet grains from the sandstones in the Kuji Group.

Formation Sample	Tm		Tm		Tm		Kn		Kn	
	S100517-2S	S100517-2S	S100517-2S	S100517-2S	S100517-2S	S100530-4S	S100522-1S	S100522-1S	S100522-2S	S100522-2S
SiO <sub>2</sub>	36.86	38.02	37.54	38.31	37.47	37.41	37.10	38.46	37.47	36.77
TiO <sub>2</sub>	0.20	0.22	0.19	0.87	0.20	0.16	0.19	0.46	0.15	0.29
Al <sub>2</sub> O <sub>3</sub>	19.68	19.91	20.30	16.77	20.09	20.12	20.09	20.29	20.50	19.92
Cr <sub>2</sub> O <sub>3</sub>	0.22	0.14	0.13	0.23	0.16	0.15	0.20	0.07	0.14	0.17
FeO*	38.18	14.98	23.70	8.60	32.87	32.24	33.86	26.09	22.44	30.28
MnO	3.13	18.99	14.19	3.71	1.01	2.69	5.45	3.38	13.87	9.80
MgO	1.01	4.56	3.07	0.00	2.31	4.64	2.37	4.86	3.79	1.82
CaO	0.66	3.11	1.13	30.96	5.49	1.67	0.56	6.47	1.40	0.82
Na <sub>2</sub> O	0.00	0.00	0.00	0.17	0.00	0.00	0.00	0.00	0.00	0.00
K <sub>2</sub> O	0.05	0.05	0.00	0.12	0.03	0.05	0.04	0.07	0.07	0.06
Total	99.99	99.98	100.25	99.74	99.66	99.14	99.85	100.15	99.85	99.93
Si	6.12	6.08	6.08	5.97	6.10	6.08	6.09	6.09	6.05	6.06
Ti	0.02	0.03	0.02	0.10	0.02	0.02	0.02	0.05	0.02	0.04
Al	3.85	3.75	3.87	3.08	3.85	3.85	3.89	3.79	3.90	3.87
Cr	0.03	0.02	0.02	0.03	0.02	0.02	0.03	0.01	0.02	0.02
Fe <sup>3+</sup>	0.00	0.03	0.00	0.81	0.00	0.00	0.00	0.00	0.00	0.00
Fe <sup>2+</sup>	5.09	1.89	3.08	0.26	4.29	4.21	4.46	3.32	2.91	4.01
Mn	0.44	2.57	1.95	0.49	0.14	0.37	0.76	0.45	1.90	1.37
Mg	0.25	1.09	0.74	0.00	0.56	1.12	0.58	1.15	0.91	0.45
Ca	0.12	0.53	0.20	5.17	0.96	0.29	0.10	1.10	0.24	0.14
Na	0.00	0.00	0.00	0.05	0.00	0.00	0.00	0.00	0.00	0.00
K	0.01	0.01	0.00	0.02	0.01	0.01	0.01	0.01	0.01	0.01
	15.92	16.00	15.95	16.00	15.95	15.97	15.93	15.97	15.97	15.97
XMg	0.04	0.18	0.12	0.00	0.09	0.19	0.10	0.19	0.15	0.07
XFe	0.86	0.31	0.52	0.04	0.72	0.70	0.76	0.55	0.49	0.67
XMn	0.07	0.42	0.33	0.08	0.02	0.06	0.13	0.08	0.32	0.23
XCa	0.02	0.09	0.03	0.87	0.16	0.05	0.02	0.18	0.04	0.02
Alm	0.86	0.31	0.52	0.04	0.72	0.70	0.76	0.55	0.49	0.67
Py	0.04	0.18	0.12	0.00	0.09	0.19	0.10	0.19	0.15	0.07
(Sp+Gro+And)	0.09	0.51	0.36	0.96	0.18	0.11	0.15	0.26	0.36	0.25
Sp	0.07	0.42	0.33	0.08	0.02	0.06	0.13	0.08	0.32	0.23
(Py+Alm)	0.91	0.49	0.64	0.04	0.82	0.89	0.85	0.74	0.64	0.75
(Gro+And)	0.02	0.09	0.03	0.87	0.16	0.05	0.02	0.18	0.04	0.02

$XMg = Mg / (Mg + Fe^{2+} + Mn + Ca)$ ,  $XFe = Fe^{2+} / (Mg + Fe^{2+} + Mn + Ca)$ ,  $XMn = Mn / (Mg + Fe^{2+} + Mn + Ca)$ ,  $XCa = Ca / (Mg + Fe^{2+} + Mn + Ca)$

$Alm = XFe$ ,  $Py = XMg$ ,  $Sp = XMn$ ,  $(Gro+And) = XCa$

Tm: Tamagawa Formation, Kn: Kunitan Formation, FeO\* is total Fe.

Table 3 Chemical composition of detrital tourmaline grains from the sandstones in the Kuji Group.

Formation Sample number	Tm	Tm	Tm	Tm	Tm	Tm	Kn	Kn	Kn	Kn
	S100517-2S tour_01	S100528-6S tour_68	S100528-6S tour_90	S100530-4S tour_107	S100530-4S tour_121	S100529-12S tour_12	S100522-1S tour_03	S100529-11S tour_38	S100529-11S tour_94	S100530-5S tour_33
SiO <sub>2</sub>	36.38	35.70	35.49	36.20	34.47	35.68	37.33	35.48	35.31	35.99
TiO <sub>2</sub>	0.79	0.84	1.53	0.74	0.06	1.87	1.47	1.06	2.51	1.95
Al <sub>2</sub> O <sub>3</sub>	31.80	28.11	30.03	29.37	25.19	29.06	29.95	33.09	25.45	29.68
Cr <sub>2</sub> O <sub>3</sub>	0.13	0.14	0.11	0.07	0.10	0.14	0.05	0.05	0.22	0.06
FeO*	4.00	8.28	8.95	10.33	15.49	8.75	7.89	9.82	10.54	6.28
MnO	0.02	0.04	0.10	0.03	0.12	0.00	0.08	0.06	0.15	0.07
MgO	8.00	7.89	5.76	6.05	5.22	6.53	7.24	3.41	7.47	8.27
CaO	1.68	3.12	1.64	1.90	2.39	2.36	1.12	0.62	0.72	2.06
Na <sub>2</sub> O	1.63	1.14	1.78	1.69	1.36	1.44	2.16	1.66	2.50	1.84
K <sub>2</sub> O	0.12	0.11	0.10	0.06	0.06	0.07	0.09	0.11	0.07	0.10
Total	84.55	85.38	85.48	86.43	84.48	85.92	87.38	85.36	84.93	86.29
Si	6.07	6.07	6.03	6.09	6.07	6.05	6.14	6.00	6.06	5.99
Ti	0.10	0.11	0.20	0.09	0.01	0.24	0.18	0.13	0.32	0.24
Al	6.26	5.63	6.01	5.83	5.23	5.81	5.80	6.60	5.15	5.82
Cr	0.02	0.02	0.01	0.01	0.01	0.02	0.01	0.01	0.03	0.01
Fe	0.56	1.18	1.27	1.45	2.28	1.24	1.08	1.39	1.51	0.87
Mn	0.00	0.01	0.01	0.00	0.02	0.00	0.01	0.01	0.02	0.01
Mg	1.99	2.00	1.46	1.52	1.37	1.65	1.77	0.86	1.91	2.05
	15.00	15.00	15.00	15.00	15.00	15.00	15.00	15.00	15.00	15.00
Ca	0.30	0.57	0.30	0.34	0.45	0.43	0.20	0.11	0.13	0.37
Na	0.53	0.38	0.59	0.55	0.46	0.47	0.69	0.54	0.83	0.59
K	0.03	0.02	0.02	0.01	0.01	0.02	0.02	0.02	0.02	0.02
B*	3.00	3.00	3.00	3.00	3.00	3.00	3.00	3.00	3.00	3.00
	18.85	18.97	18.91	18.91	18.93	18.92	18.90	18.68	18.98	18.98

Tm: Tamagawa Formation, Kn: Kunitan Formation, FeO\* is total Fe. B\* is assuming 3 p.f.u.

Table 4 Chemical composition of detrital chromian spinels from the sandstones in the Kuji Group.

Formation Sample number	Tm	Kn	Kn								
	S100517-2S	S100517-2S	S100517-2S	S100517-2S	S101120-1S	S100530-4S	S100530-4S	S100530-4S	S100530-4S	S100522-2S	S100522-2S
	pico_18	pico_41	pico_79	pico_89	pico_66	pico_61	pico_62	pico_63	pico_106	pico_58	pico_74
TiO <sub>2</sub>	0.44	2.03	0.66	0.49	0.55	0.57	0.74	0.73	0.61	2.67	0.67
Al <sub>2</sub> O <sub>3</sub>	9.73	20.63	7.40	9.70	9.38	9.57	10.57	17.26	9.82	21.22	26.21
FeO*	25.87	26.04	35.33	24.24	29.91	29.72	34.93	20.47	29.21	24.70	19.91
MnO	1.17	0.71	1.02	1.15	0.91	1.10	1.23	0.84	0.91	0.91	0.61
MgO	9.49	13.28	6.30	9.97	6.75	7.55	5.45	13.20	8.31	12.21	12.91
Cr <sub>2</sub> O <sub>3</sub>	51.64	36.97	49.35	53.64	51.35	51.00	46.50	47.37	50.30	37.55	38.81
Total	98.34	99.66	100.07	99.19	98.85	99.52	99.43	99.87	99.17	99.27	99.13
Al	3.08	6.00	2.38	3.04	3.02	3.04	3.39	5.09	3.11	6.23	7.53
Cr	10.96	7.21	10.64	11.27	11.08	10.86	10.01	9.38	10.68	7.40	7.48
Fe <sup>3+</sup>	1.82	2.05	2.75	1.52	1.70	1.89	2.34	1.28	2.00	1.39	0.78
Ti	0.09	0.38	0.14	0.10	0.11	0.12	0.15	0.14	0.12	0.50	0.12
Mg	3.80	4.89	2.56	3.95	2.75	3.03	2.21	4.93	3.33	4.53	4.69
Fe <sup>2+</sup>	3.99	3.33	5.30	3.86	5.12	4.80	5.61	3.00	4.56	3.76	3.27
Mn	0.27	0.15	0.24	0.26	0.21	0.25	0.28	0.18	0.21	0.19	0.13
	24.00	24.00	24.00	24.00	24.00	24.00	24.00	24.00	24.00	24.00	24.00
Mg/(Mg+Fe <sup>2+</sup> )	0.49	0.59	0.33	0.51	0.35	0.39	0.28	0.62	0.42	0.55	0.59
Cr/(Cr+Al)	0.78	0.55	0.82	0.79	0.79	0.78	0.75	0.65	0.77	0.54	0.50
Ycr	0.69	0.47	0.67	0.71	0.70	0.69	0.64	0.60	0.68	0.49	0.47
YFe <sup>3+</sup>	0.11	0.13	0.17	0.10	0.11	0.12	0.15	0.08	0.13	0.09	0.05
YAl	0.19	0.39	0.15	0.19	0.19	0.19	0.22	0.32	0.20	0.41	0.48

Ycr=Cr/(Cr+Al+Fe<sup>3+</sup>), YFe<sup>3+</sup>=Fe<sup>3+</sup>/(Cr+Al+Fe<sup>3+</sup>), YAl=Al/(Cr+Al+Fe<sup>3+</sup>)

Tm: Tamagawa Formation, Kn: Kunitan Formation, FeO\* is total Fe.